# EVOLUTIONARY GAME THEORY AND THE SPREAD OF INFLUENZA

By
Marc A. Beauparlant

A Thesis
submitted to the School of Graduate Studies and Research
in partial fulfillment of the requirements
for the degree of
Master of Science in Mathematics[1]



[1]The M.Sc. Program is a joint program with Carleton University, administered by the Ottawa-Carleton Institute of Mathematics and Statistics

# Abstract

Vaccination has been used to control the spread of infectious diseases for centuries with widespread success. Deterministic models studying the spread of infectious disease often use the assumption of mass vaccination; however, these models do not allow for the inclusion of human behaviour. Since current vaccination campaigns are voluntary in nature, it is important to extend the study of infectious disease models to include the effects of human behaviour. To model the effects of vaccination behaviour on the spread of influenza, we examine a series of models in which individuals vaccinate according to memory or individual decision-making processes based upon self-interest. Allowing individuals to vaccinate proportionally to an exponentially decaying memory function of disease prevalence, we demonstrate the existence of a Hopf bifurcation for short memory spans. Using a game-theoretic influenza model, we determine that lowering the perceived vaccine risk may be insufficient to increase coverage to established target levels. Utilizing evolutionary game theory, we examine models with imitation dynamics both with and without a decaying memory function and show that, under certain conditions, periodic dynamics occur without seasonal forcing. Our results suggest that maintaining diseases at low prevalence with voluntary vaccination campaigns could lead to subsequent epidemics following the free-rider dilemma and that future research in disease control reliant on individual-based decision-making need to include the effects of human behaviour.

# Acknowledgements

I would first like to thank Dr. Robert Smith? for all of his guidance, support, encouragement and for being my patient zero by successfully infecting me with the need to study infectious disease modeling. You have taught me more than I could have ever imagined and I am so very thankful for having the opportunity to work with you over the past few years. I would also like to thank Dr. Smith? for being aware of the mental health of his students and taking away from the negativity that often accompanies academia. Graduate students often feel like impostors, but he always reminded us of why we belong exactly where we are.

I would like to thank all of my family and friends for all their love, help and support. To my Mom, thank you for always listening when I needed it most and encouraging me to keep moving forward one step at a time. I could not have made it this far without you. To my Dad, thank you for teaching me to take time away from my studies to recharge my batteries. To my Sister, thank you for always making me laugh and smile. You always know how to brighten my day. To my Cousin, thank you for helping me build my self-confidence and putting up with my math-talk (let's be honest, you were interested in at least one out of those million conversations). Last but not least, thank you to all of my friends for ensuring my social life did not die completely during grad school.

# Dedication

I dedicate this work to my sister's children Pero, Adrijana and Ilija. I love you three to the moon and back.

# Contents

**Abstract** **ii**

**Acknowledgements** **iii**

**Dedication** **iv**

**1 Introduction** **1**

**2 Deterministic models with waning immunity** **10**

2.1 Lyapunov Stability Theory . . . . . 11

2.2 Analysis . . . . . 15

**3 Memory** **20**

3.1 Model assumptions and governing equations . . . . . 21

3.2 Analysis . . . . . 22

3.3 Numerical Simulations . . . . . 28

3.3.1 Sensitivity Analysis . . . . . 31

3.4 Discussion . . . . . 37

**4 Game Theory** **38**

4.1 The epidemiological model . . . . . 39

4.2 Game-theoretic model . . . . . 42

4.3 Numerical simulations . . . . . 45

4.4 Discussion . . . . . 46

**5 Evolutionary Game Theory** **49**
5.1 Model with Imitation Dynamics . . . . . 53
5.2 Analysis . . . . . 55
5.3 Numerical Simulations and Analysis . . . . . 61
5.3.1 Simulations without waning immunity: exploration of imitation parameters . . . . . 61
5.3.2 Simulations with waning immunity . . . . . 65
5.3.3 Numerical Analysis using Lyapunov Exponents . . . . . 66
5.3.4 Sensitivity Analysis . . . . . 68
5.4 Discussion . . . . . 70

**6 Imitation dynamics with memory** **77**
6.1 Model assumptions and equations . . . . . 77
6.2 Analysis . . . . . 79
6.3 Numerical simulations and sensitivity analysis . . . . . 82
6.3.1 Numerical simulations . . . . . 82
6.3.2 Sensitivity Analysis . . . . . 85
6.4 Discussion . . . . . 87

**7 Results, conclusions and future work** **90**

# Chapter 1

# Introduction

Influenza is an infectious disease caused by the influenza virus from the family *Orthomyxoviridae*. The virus is spread from person to person through droplets created while coughing, sneezing or talking, which enter a susceptible individual through the eyes, nose or mouth. Although individuals need to be in close proximity to spread the virus, it is also spread by touching contaminated surfaces and then touching the eyes, nose or mouth. Once infected, individuals may become contagious up to a day before presenting any symptoms and may spread the disease for up to a week after becoming ill [7]. Influenza manifests itself through four main subtypes: A, B, the lesser-known C and a proposed new variant D. The most dangerous strains are of type A causing the highest amount of morbidity and mortality, which have been responsible for several major global pandemics such as the Spanish flu of 1919, which is estimated to have caused between 20 to over 50 million deaths worldwide [42]. Other notable pandemic outbreaks of influenza include the Asian flu (1957–58), and the Hong Kong flu (1968–69) which caused over a million global deaths each. In more recent history, the swine flu outbreak (H1N1) of the 2009–2010 season was much less severe than expected in developed countries; however, it still managed to cause between 151,700 and 575,400 deaths, with half of these having occurred in African and Southeast Asian regions [10].

Humans are the main reservoir for influenza A viruses; however, the virus circulates through wild bird populations such as ducks and geese, as well as in pigs. It is

suspected that animal reservoirs are sources of new human subtypes, and zoonosis has been documented from pigs and fowl to humans [32]. Of particular concern are confined animal feeding operations (CAFOs) which have been shown to increase the risk of zoonotic infection of influenza in CAFO workers for both avian and swine species [26, 37]. With the large number of animals in these farms and frequent outbreaks among these animals, the virus has many opportunities to undergo antigenic shift. This leads to a higher probability of producing a new variant that is able to spread from human to human. It has also been suggested that CAFOs act as amplifiers for influenza and that annually vaccinating half of all CAFO workers would cancel this amplification [37]. Vaccination is therefore not only a method to slow the epidemic spread of seasonal influenza but also as a way to reduce the probability of contracting new variants of the influenza virus from animal reservoirs.

Mass influenza vaccination began in 1945 in the United States. Since then, the flu vaccine has been used globally to reduce the risks of morbidity and mortality caused by influenza infection. The Centers for Disease Control and Prevention (CDC) recommends vaccinating elderly persons (65+) and any young children or high-risk individuals [7]. The first country to change legislation to include vaccination of schoolchildren against influenza was Japan from 1962–1987 following the pandemic Asian flu of 1957, becoming mandatory in 1977. The reason for this change was because schoolchildren are the primary spreaders of the disease [35]. Mathematical models have suggested that a high vaccination rate of schoolchildren would significantly reduce the impact of influenza on the community. During the implementation of this program, Japan had a marked reduction in excess deaths attributed to influenza and pneumonia, especially among the elderly; approximately one death was prevented for every 420 schoolchildren vaccinated. Vaccination of schoolchildren was however halted in 1994 due to growing public doubts in its effectiveness and through lawsuits alleging adverse side effects. Following the discontinuation of the program, vaccine coverage dropped to low levels, and excess deaths increased sharply in the first year without program [35]. Mistrust is considered to be partly due to studies analyzing the reduction of

morbidity and mortality in schoolchildren and did not focus on the secondary protection that was provided to the elderly. It is important to note that implementing a national mandatory vaccination program against influenza in schoolchildren would most likely come with stern opposition, and if implemented, we would expect to see a similar loss in trust of vaccine effectiveness and increased reporting in adverse vaccine side effects. Growing mistrust in one vaccine could also lead to mistrust in vaccines in a general manner, negatively affecting other successful vaccination programs.

Current vaccines work by generating an immune response in the host against Haemagglutinin (HA) and Neuraminidase (NA) (two glycoproteins found in abundance on the surface of the virus) [49]. The difficulty of adequately protecting the population from influenza with vaccination is due to the rate at which the virus mutates through the processes of antigenic shift and drift. Antigenic drift occurs in all strains of influenza and is the natural mutation accumulated by the genome of the virus that codes for antibody binding sites [41]. Once the antigen is sufficiently different from the antigen recognized by the immune system, it will be able to evade immune response, potentially leading to an outbreak. In contrast, antigenic shift leads to significant genetic changes in a rapid manner. Occurring only in influenza A, antigenic shift occurs when two or more different strains of the virus combine to create a novel influenza A virus. These changes are more abrupt and leave the human population more susceptible to infection. The reason influenza types B and C do not undergo antigenic shift is due to the fact they primarily infect human populations [50], while influenza A viruses infect a broader range of mammalian and avian hosts, increasing the probability of reassortment [41]. The evolution of the influenza virus from season to season through shift and drift make it difficult to create a vaccine that remains effective for multiple seasons. The ability of influenza to consistently evade our infection-and vaccine-induced immunities makes the virus particularly difficult to eradicate. It has been suggested that, with or without a universal flu vaccine, the disease may be impossible to eradicate due to difficulties with adherence [43]. Problems with population adherence to influenza vaccination are due to the complex interplay between their perceived costs of infection, vaccination, societal and religious beliefs, peer influence or recommendation from health-care professionals [13, 22, 29].

The spread of diseases such as influenza can be studied through the use of compartmental models, originally implemented by Kermack and McKendrick [18]. Essentially, the population is divided into distinct classes based on their infection status and transition through these states under certain assumptions based on the properties of the disease studied. As an example, suppose a disease provides life-long immunity after infection. Individuals begin in the susceptible class ($S$) where they are equally susceptible to infection. Individuals get infected through contact with an infected individual at some rate (generally denoted by $\beta$), which moves them to the infected class ($I$). Individuals will remain infectious for a certain period of time ($\frac{1}{\gamma}$ days) and then will be moved to the recovered class ($R$). Adding a constant birth rate $\Lambda$ and death rate proportional to population size $\mu$ adds in the effects of demography. The above description corresponds to the Susceptible-Infected-Recovered (SIR) model illustrated in Figure 1. This model can be built upon to accommodate different properties of a disease. For a disease with waning immunity, individuals will move back to the susceptible class, corresponding to a Susceptible-Infected-Recovered-Susceptible (SIRS) model (discussed in more detail in Chapter 2). Diseases may also have an incubation period where an individual is infected but not yet infectious (an exposed individual). Including this intermediate class between the susceptible and infectious classes, we obtain the Susceptible-Exposed-Infected-Recovered (SEIR) model. To model the effects of vaccination, a vaccinated class can be included where individuals are immune (or partially immune) to infection, corresponding to a Susceptible-Infected-Recovered-Vaccinated (SIRV) model. Other properties such as age-structure, disease-related mortality and quarantine could be added to better study the spread of disease or the efficacy of control measures.

The complex nature of vaccination decisions cannot be effectively studied using simple compartmental models. Coupling these epidemic models with game theory and evolutionary game theory allow for the study of vaccine free-riding [1, 2, 3, 4, 13, 24, 27, 28, 31, 45, 48]. Individuals free-ride on herd immunity conferred by the vaccination of a critical number of individuals in their vicinity. In classic game theory applied to a vaccination game, an individual will choose a strategy to vaccinate based on the perceived costs of vaccination, infection and on the strategies chosen by the

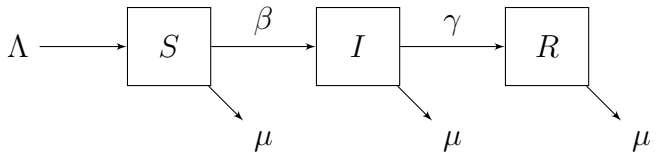


Figure 1: Flow of a compartmental Susceptible-Infected-Recovered (SIR) model. Parameters and states are defined in Table 1

remainder of the population. The goal of these models is to determine the strategy that provides an individually optimal payoff: the Nash equilibrium. In evolutionary game theory, individuals are able to update their strategies to create a more dynamic game. Using imitation dynamics, individuals can update their strategy over time by imitating a strategy with higher payoff. In these models, we seek an Evolutionary Stable Strategy (ESS) where no other strategy introduced at low levels would provide a higher payoff. These concepts will be discussed in greater detail in Chapters 4 and 5.

Bauch and Earn [3] studied a game-theoretic model for a childhood disease to aid in the development of childhood vaccination policy. The authors use a simple SIR model to determine the probability of infection in order to quantify the risks of infection. It was found that, for any relative risk of infection versus vaccination, the Nash equilibrium for vaccination was below the critical vaccination threshold for herd immunity. Furthermore, by analyzing the payoff changes as the relative risk is varied, it was found that the vaccination uptake is much more sensitive to negative factors such as vaccine scares than it is to positive factors such as education campaigns. This occurs because the incentive to decline vaccination remains substantial even as vaccination coverage approaches low levels. In contrast, the incentive to vaccinate decreases as the population approaches the Nash equilibrium. This means that it is much easier for vaccination coverage to drop following a vaccine scare or any other negative factors, and it will be relatively difficult to restore higher levels of vaccination coverage afterwards. This study suggests that there are added difficulties for public-health officials when individuals make choices under a voluntary vaccination policy (especially as the perceived risk of infection is lowered). This study substantiates the

need for studying models throughout the course of the whole vaccination campaign with emphasis on when the disease is near eradication, since the perceived risk of infection should be significantly lowered.

In the game-theoretic model proposed for childhood diseases by Bauch and Earn [3], it was possible to carry out analysis of the stability of the Nash equilibrium and showed that is was a convergently stable Nash equilibrium. Carrying out the analysis of stability for the Nash equilibrium and determining it becomes increasingly difficult as population heterogeneity is introduced into models. For example, perceptions of risk of influenza increase significantly with age. It is therefore expected that elderly individuals will have different vaccination strategies than those who are less at risk. Galvani et al.[13] constructed a two-age model for influenza using game theory. Since analysis cannot be carried out to determine convergently stable Nash equilibria directly, the authors developed a Monte Carlo algorithm to calculate the proportion of individuals vaccinating at equilibrium in both age classes. What was found was that levels of vaccination coverage were below the community optimum when individuals vaccinated according to self-interest. Consequently, elderly individuals at higher risk vaccinated with higher probability than young individuals following current vaccination policies. The authors highlight that the discrepancy may be caused by an inflated sense of attack risk, speed of spread or a distorted impression of transmission potential, health interventions and the probability of being infected.

The probability of infection for influenza is also often overestimated due to influenza-like illness (ILIs), which increase the perceived incidence of infection among the population. A similar result of the discrepancy between the self-and group-interest was found in models studying vaccination against smallpox following a potential bioterrorist attack [4]. This shows an inherent need to fully study the effects of human infection risk assessment and consequent vaccination behaviour. Although game theory is well-suited to study these effects, the static nature of risk evaluation does not allow for perceptions of infection and vaccine risk to evolve over time. As an example, vaccination programs and adherence in Japan increased sharply following the Asian

flu epidemic and subsequently decreased as the infection risk was decreased. Evolutionary game theory provides a natural framework to study the more dynamic interaction of individuals' vaccination decisions. This can be done by allowing individuals to sample from a set of available strategies and switch to strategies which are more advantageous. Poletti et al.[31] considered such a model for the 2009 H1N1 pandemic in Italy in which individuals altered their behaviour based on the perceived risks/costs of influenza infection and vaccination. The authors suggest that the severity of the pandemic may have been mitigated in Italy due to spontaneous behavioural changes to self-protective behaviours such as hand-washing or social distancing. D'Onofrio et al. [27] proposed a model using imitation dynamics in an attempt to measure the impact of vaccine side effects (VSEs) on the history of vaccination programs. It was found that imitation dynamics led to complex dynamics with oscillations when considering a linear increase in vaccine risk due to reporting of VSEs. This is due to the negative feedback caused by an increase in vaccination. When disease prevalence is high, vaccination increases (reducing disease prevalence), and subsequently the number of reported VSEs increases, which leads to a drop in vaccination coverage. The authors also studied the effects of a time-delay on the reporting of VSEs, as they may take time to be observed and/or reported. It was found that the time-delay in reporting VSEs has cumulative effects, with the imitation dynamics leading to instability of one of the endemic equilibria, resulting in persistent oscillations. The authors went on to suggest that industrialized countries could face serious difficulties in maintaining vaccination uptake, as the perceived risk of infection continues to decrease for many diseases from decades of successful vaccination programs. Special care will need to be taken as diseases reach the eradication threshold globally as vaccination rates are expected to decline.

Bauch has several papers studying the effects of imitation dynamics on the spread of infectious diseases [1, 2, 24]. In his 2013 paper [1], Bauch built an SIR model with imitation dynamics for a disease in which children are vaccinated at birth depending on the parents' views on vaccination, which are modeled using imitation dynamics. It was found that the dynamics of this model were able to reproduce features observed for pertussis vaccine uptake in England and Wales during the 1970s. The features

observed include the oscillations in vaccination uptake as a response to the natural oscillatory nature of disease outbreaks and the relatively slow recovery of vaccination uptake following a vaccination scare. Again, this substantiates the need to include game theory as a tool in disease modeling to better understand the effects of voluntary vaccination campaigns on the control of infectious diseases. The authors also noted that high vaccination coverage in countries should not be taken for granted.

In the following chapters, we will explore models for influenza that allow individuals to base vaccination decisions on risks of vaccination as well as the risk of infection with current and past infection prevalence. The chapters are organized as follows. Chapter 2 is dedicated to introducing compartmental deterministic SIRV models with waning immunity. A modification of a Lyapunov stability theory proof for equilibrium points is added to allow for simple Lyapunov functions for the models studied. Global stability of the disease-free and endemic equilibria will be proven using Lyapunov stability theory, which will also be applied to models in later chapters. Chapter 3 introduces a modified SIRV model where individuals vaccinate in proportion to the prevalence of infection over a certain number of seasons through a decaying memory function. This model is a precursor to the game-theoretic models presented in subsequent chapters. Analytic proof of a Hopf bifurcation will be shown to occur for this simple model. In Chapter 4, models created by Bauch and Earn [3] are modified using a different vaccination structure in order to adapt the vaccination game from smallpox to influenza. This chapter also serves as an introduction to the use of payoff functions, which will be used in subsequent chapters. Chapter 5 analyzes the SIRV model with imitation dynamics similar to the papers mentioned above. This chapter will show that imitation dynamics are also sufficient to illicit periodic dynamics from the underlying SIRV model when individuals vaccinate using short-sighted behaviour. Chapter 6 integrates the decaying memory function and the imitation dynamics to show that periodic dynamics may occur for longer memory spans so long as the risk of vaccination is sufficiently low. We will conclude with a statement of results and discuss directions for future work.

Table 1: Description of all parameters, state variables and equilibrium notation for all models studied. Compartment state variables $(S, I, R, V, M, x)$ at equilibrium are given the associated subscripts and superscripts.

| | Description | Units |
|---|---|---|
| $N$ | Total number of individuals | people |
| $S$ | Number of susceptible individuals | people |
| $I$ | Number of infected individuals | people |
| $R$ | Number of recovered individuals | people |
| $V$ | Number of vaccinated individuals | people |
| $M$ | Number of infected individuals in $\theta$ seasons | people |
| $x$ | Proportion of individuals actively seeking vaccination | |
| $X_0$ | Non-vaccinator disease-free equilibrium | people |
| $X_0^*$ | Pure-vaccinator disease-free equilibrium | people |
| $X_E$ | Mixed-strategy endemic equilibrium | people |
| $X_E^*$ | Non-vaccinator endemic equilibrium | people |
| $\bar{X}_E$ | Pure-vaccinator endemic equilibrium | people |
| $\Lambda$ | Human birth rate | people $\text{days}^{-1}$ |
| $\mu$ | Human death rate | $\text{days}^{-1}$ |
| $\beta$ | Contact rate | $\text{people}^{-1}\text{days}^{-1}$ |
| $\gamma$ | Recovery rate | $\text{days}^{-1}$ |
| $\psi$ | Infection-induced immunity waning rate | $\text{days}^{-1}$ |
| $\phi$ | Vaccine-induced immunity waning rate | $\text{days}^{-1}$ |
| $\theta$ | Number of seasons in the memory span | |
| $\rho$ | Vaccination rate | |
| $r_i$ | Scaled risk of infection | |
| $r_v$ | Scaled risk of vaccination $(1 - r_i)$ | |
| $k$ | Mixed imitation rate | $\text{days}^{-1}$ |

# Chapter 2

# Deterministic models with waning immunity

The use of compartmental models to study the spread of epidemics was first introduced by Kermack and McKendrick [18]. Under certain assumptions, the spread of disease through a population may be studied using ordinary differential equations. The population is generally divided into susceptible, infected and removed (recovered) compartments, where susceptible individuals are equally susceptible to infection. Additional compartments may be included to more closely resemble the dynamics of a disease such as a latent class (exposed), where individuals are infected but not yet infectious, or infected but asymptomatic. A classic and well-studied example is the $SIR$ model where individuals obtain permanent immunity following infection. The $SIR$ model and variants of this model (such as the inclusion of age structure, seasonality, demography and other population heterogeneities) have been used to study the spread of influenza [13, 14, 21]. Unfortunately, the solution to the system of equations described by the $SIR$ model cannot generally be expressed in closed form. Although this limits the ability for these systems to be analyzed, other tools such as stability analysis using the linearized system provide sufficient information to determine stability of equilibria without solving. Increasing the complexity of an $SIR$ model may therefore only provide insight to the stability of equilibria. This limits

the capability to create models that are representative of the spread of a specific disease; however, these simplified models can provide important conclusions regarding the disease dynamics.

Once a susceptible individual becomes infected with influenza, they only acquire immunity to the strain that infected them. Individuals are therefore susceptible to influenza in the following season when a mutated strain becomes dominant through antigenic shift or drift. By including waning immunity, we obtain an $SIRS$ model. The governing system of ordinary differential equations is again unsolvable, and determining the global stability of equilibrium points becomes increasingly difficult. In this section, we will study the dynamics of the $SIRS$ models using Lyapunov stability theory. For global stability of the disease-free equilibrium, a simple Lyapunov function is used in some papers that does not satisfy certain conditions outlined in Lyapunov's stability theorem; we will go on to justify the use of this Lyapunov function to show that the disease-free equilibrium is globally asymptotically stable for all systems of a certain family, which includes all those discussed in later chapters. This chapter will first discuss Lyapunov stability theory and then apply these results to a simple SIRS model.

## 2.1 Lyapunov Stability Theory

Lyapunov's stability theorem is a powerful result in mathematics, but finding an appropriate Lyapunov function (defined below) is notoriously difficult. We begin this section with a definition of a Lyapunov candidate function and Lyapunov's stability theorem [19].

**Definition 2.1.1.** For a system of ordinary differential equations $\mathbf{x}' = F(\mathbf{x})$ with $\mathbf{x} \in \mathbb{R}^n$ and equilibrium point $\mathbf{x_0}$, a Lyapunov candidate function $L : \mathbb{R}^n \to \mathbb{R}$ is a *locally positive-definite function*:

1. $L(\mathbf{x_0}) = 0$
2. $L(\mathbf{x}) > 0 \ \forall x \in \mathbb{R}^n \backslash \{\mathbf{x_0}\}$.

**Theorem 2.1.2.** *The equilibrium* $\mathbf{x_0}$ *of the n-dimensional dynamical system* $\mathbf{x} = F(\mathbf{x})$ *is globally asymptotically stable if there exists a Lyapunov candidate function L with the following properties:*

- *L is globally positive definite:*

$$L(\mathbf{x}) > 0 \quad \forall \mathbf{x} \in \mathbb{R}^n \backslash \{\mathbf{x_0}\},\ L(\mathbf{x_0}) = 0$$

- *The time derivative of L is globally negative definite:*

$$L'(\mathbf{x}) < 0 \quad \forall \mathbf{x} \in \mathbb{R}^n \backslash \{\mathbf{x_0}\},\ L'(\mathbf{x_0}) = 0$$

- *L is radially unbounded:*

$$||\mathbf{x}|| \to \infty \implies L(\mathbf{x}) \to \infty.$$

It is important to ensure that all conditions of Lyapunov's theorem are respected, which is not always done in practice. For example, it initially seems appropriate to choose $L(S, I, R) = \frac{1}{2}I^2$ for a simple $SIR$ or $SIRS$ model. Although this choice of $L$ is radially unbounded with globally negative-definite time derivative, it is not globally positive-definite. Along the axis $I = 0$, we have $L = 0$. Therefore it is not sufficient to consider this Lyapunov function as a full proof for global stability of disease-free equilibria (DFE) for certain models such as system (1) in Section 2.2. We will show how to complete the proof using this function for the disease-free equilibrium of an $SIRS$ model by modifying a proof method outlined in Lamponi [34], extending the admissibility of simpler Lyapunov functions for certain models. We will also use a corrected Lyapunov function, originally described by Lotka & Volterra for the endemic equilibrium that previously used for ecology but which is now widely used in epidemiological contexts.

**Definition 2.1.3.** An equilibrium point $x_e$ of a nonlinear system $\mathbf{x}' = f(\mathbf{x})$ is said to be *stable* if, for all $\epsilon > 0$, there exists $\delta > 0$ such that

$$x_0 \in \mathcal{B}(x_e, \delta) \implies \varphi(t; 0, x_0) \in \mathcal{B}(x_e, \epsilon), \quad \forall t \geq 0,$$

where $\varphi(t; t_0, x_0)$ is a solution to the system with initial condition $(t_0, x_0)$.

**Theorem 2.1.4.** *Suppose an $n$-dimensional system has a unique disease-free equilibrium $x_e$. Assume there exists a Lyapunov function $L : \mathbb{R}^n_+ \to \mathbb{R}$ and $U \subset \mathbb{R}^n_+$ such that:*

1. *$L$ is positive semi-definite*
   - *$L(x) = 0$ for $x^* \in U$ (where $x_0 \in U$) and $L(x) > 0$ for $x \in \mathbb{R}^n_+ \backslash U$.*
2. *The time derivative of $L$ is negative semi-definite in the above sense.*
3. *All solutions become trapped in a bounded space as $t \to \infty$.*
4. *The equilibrium point $x_e$ is globally asymptotically stable in $U$.*

*Then $x_e$ is globally asymptotically stable in the positive orthant.*

*Proof.* We will show that solutions approach the space $U$ asymptotically. First, we use the fact that all solutions enter a bounded trapping region as $t$ increases; we may therefore only consider the subspace $U^*$ of the solution space, which is both closed and bounded. This allows us to construct the following bounded set:

$$\Omega_\epsilon = \bigcup_{x \in U^*} \mathcal{B}(\epsilon, x), \quad \epsilon > 0,$$

where $\mathcal{B}(\epsilon, x)$ denotes the $n$-ball of radius $\epsilon$ centered at $x$. Since the boundary $\partial\Omega_\epsilon$ is compact (closed and bounded) with $L$ continuous, $L$ admits a minimum $m$ on $\partial\Omega_\epsilon$ (Weierstrass [36]). Since $L$ is positive-definite on $\Omega_\epsilon \backslash U^*$, we have that

$$\min_{x \in \partial\Omega_\epsilon} L(x) = m > 0.$$

By continuity of $L$, there exists $\delta > 0$ such that

$$x_0 \in \Omega_\delta \implies |L(x_0) - L(x_e)| = L(x_0) < m.$$

Next, suppose in order to obtain a contradiction that a trajectory $\varphi(t; 0, x_0)$ starting in $\Omega_\delta$ is not contained in the region $\Omega_\epsilon$. Then there must exists some time $T$ where the trajectory intersects the boundary of $\Omega_\epsilon$. This implies that $L(\varphi(T; 0, x_0)) \geq m$.

Since the time derivative of $L$ is assumed to be negative-definite, $L$ is non-increasing along this trajectory ($L(\varphi(T;0,x_0)) \leq L(x_0)$). Therefore

$$m \leq L(\varphi(T;0,x_0)) \leq L(x_0) < m,$$

which is a contradiction. We conclude that solutions must be contained in the region $\Omega_\epsilon$. We have shown that $\forall \epsilon > 0$, there exists $\delta > 0$ such that if $x_0 \in \Omega_\delta$, then $\varphi(t;0,x_0) \in \Omega_\epsilon$ for all $t \geq 0$.

We will show that solutions approach $U$ asymptotically ($\lim_{t\to\infty} \varphi(t;0,x_0) \in U$). In other words, for all $\epsilon'$ such that $0 < \epsilon' < \epsilon$, there exists some time $T$ such that $\varphi(t;0,x_0) \in \Omega_{\epsilon'}$ for all $t \geq T$. From the stability of $U$ and time invariance, we have that for all $\epsilon' > 0$, there exists a $\delta' > 0$ such that if $x(T) \in \Omega_{\delta'}$, then $\varphi(t;T,x(T)) \in \Omega_{\epsilon'}$ for all $t \geq T$. There is therefore only the need to prove that there exists a $T$ such that $x(T) \in \Omega_{\delta'}$.

Suppose by contradiction that trajectories never enter $\Omega_{\delta'}$. Then for all $t \geq 0$, we have

$$\varphi(t;0,x_0) \in \Omega_\epsilon \backslash \Omega_{\delta'}.$$

Since $\Omega_\epsilon \backslash \Omega_{\delta'}$ is compact with $L'$ continuous and negative-definite, $L'$ attains a negative maximum $-\mu$. Therefore

$$L'(x) \leq -\mu \text{ if } x \in \Omega_\epsilon \backslash \Omega_{\delta'}.$$

Finally,

$$\begin{aligned} L(\varphi(t;0,x_0)) &= L(x_0) + \int_0^t L'(\varphi(\tau;0,x_0))d\tau \\ &\leq L(x_0) - \mu t. \end{aligned}$$

This is a contradiction, since $L$ is positive semi-definite in $\Omega_\epsilon$, while the right-hand side of the above equation tends to $-\infty$ as $t \to \infty$. Therefore there must exist $T$ such that $x(T) \in \Omega_{\delta'}$. We conclude that solutions approach the set $U$ asymptotically.

It follows that if there exists $x^* \in U$ such that $\lim_{t\to\infty} \varphi(t;0,x_0) = x^*$ with $x_0 \in U$, then $x^*$ is globally asymptotically stable. In the models studied, the set

$U$ will contain a unique disease-free equilibrium, and therefore we must have that $\lim_{t\to\infty} \varphi(t; 0, x_0) = x_e$. The disease-free equilibrium is therefore globally asymptotically stable. □

The above proof is used in later chapters to simplify the use of Lyapunov stability for disease-free equilibrium points. If there are several disease-free equilibria, extra care must be taken when using this result, which will be discussed in the proofs for later chapters. In the next section, we will apply the results of Theorem 2.1.4 to the $SIRS$ model and complete the analysis of all equilibrium points.

## 2.2 Analysis

We will now apply the result from the previous section to an $SIRS$ model. In these models, there is a replenishing of the susceptible pool, which allows for subsequent but less severe epidemic peaks. Solutions to this system are oscillatory in nature but eventually converge asymptotically to either the endemic equilibrium or the disease-free equilibrium. It is important to note that the $SIR$ model is just a rescaled version of the $SEIR$ model, and we will therefore reduce the burden of analysis by considering the $SIR$ model for the majority of the systems in later chapters. This is equivalent to the assumption that exposed individuals are immediately infectious. Although this assumption does not reflect the nature of influenza, we will draw important conclusions in later chapters from this minor simplification. A traditional $SIRS$ model is given below in system (1). In this model, we will make the following assumptions:

1. Individuals die at constant rate $\mu$, independent of infection status, and are born at constant rate $\Lambda = N \cdot \mu$ to ensure an asymptotically constant population size.

2. Susceptible individuals ($S$) become infected following contact with an infectious individual at rate $\beta$ through frequency-dependent transmission.

3. Infected individuals ($I$) recover from infection at rate $\gamma$, moving to the recovered ($R$) class.

4. Recovered individuals maintain immunity from infection temporarily, moving to the susceptible class with immunity waning at rate $\psi$ (individuals maintain immunity for $\frac{1}{\psi}$ days).

The model is thus given by

$$\begin{aligned} S' &= \Lambda - \mu S - \frac{\beta SI}{N} + \psi R \\ I' &= \frac{\beta SI}{N} - \mu I - \gamma I \\ R' &= \gamma I - (\mu + \psi) R. \end{aligned} \tag{1}$$

**Proposition 2.2.1.** *The unique disease-free equilibrium given by*

$$X_0 = (S_0, I_0, R_0) = \left(\frac{\Lambda}{\mu}, 0, 0\right)$$

*is globally asymptotically stable if* $\mathcal{R}_0 = \frac{\beta}{\mu+\gamma} < 1$.

*Proof.* We propose the Lyapunov function $L = \frac{1}{2}I^2$ to determine stability of $X_0$. First, we have that $L$ is positive semi-definite in the sense of Theorem 2.1.4, where $U = \{x \in \mathbb{R}_0^{3+} | I = 0\}$. The time derivative is given by

$$L' = I \cdot I' = I^2 \left(\frac{\beta S}{N} - \mu - \gamma\right) < 0 \text{ for } I \neq 0 \text{ and } \mathcal{R}_0 = \frac{\beta}{\mu + \gamma} < 1.$$

The time derivative of $L$ is therefore negative semi-definite in the sense of Theorem 2.1.4. Next, we must show that all solutions eventually enter some bounded space. This is ensured by the asymptotically constant population of system (1). By adding all equations, we have $N' = \Lambda - \mu N$ and therefore $\lim_{t\to\infty} N(t) = \frac{\Lambda}{\mu}$. Hence solutions eventually enter the bounded region $\{(S, I, R) \in \mathbb{R}_0^{3+} | S + I + R \leq \frac{\Lambda}{\mu}\}$. We will finally show that the disease-free equilibrium is globally asymptotically stable in $U = \{x \in \mathbb{R}_0^{3+} | I = 0\}$. When $I = 0$, we have $R' = -(\mu + \psi)R < 0$ and thus $\lim_{t\to\infty} R = 0$. It follows that

$$\lim_{t\to\infty} S(t) = \lim_{t\to\infty} N - I - R = \frac{\Lambda}{\mu}.$$

Therefore all solutions with initial conditions in $U$ approach $X_0$ as $t \to \infty$. Hence $X_0$ is globally asymptotically stable in $U$ and, from Theorem 2.1.4, is globally asymptotically stable in the positive orthant.

□

In the other systems in subsequent chapters, there are multiple disease-free equilibrium points, which requires modification of the above theorem. Special care must be taken when using positive semi-definite Lyapunov functions with Theorem 2.1.4 as the results of Lyapunov's Stability Theorem are only applicable for positive definite Lyapunov functions.

**Proposition 2.2.2.** *The endemic equilibrium $X^*$ is given by*

$$X^* = (S^*, I^*, R^*) = \left( \frac{\Lambda(\mu+\gamma)}{\mu\beta}, \frac{\Lambda(\mu+\psi)(\beta-\mu-\gamma)}{\mu\beta(\mu+\psi+\gamma)}, \frac{\Lambda\gamma(\beta-\mu-\gamma)}{\mu\beta(\mu+\psi+\gamma)} \right)$$

*is globally asymptotically stable whenever $I_0 \neq 0$.*

*Proof.* We will show that the Lyapunov function proposed by O'Regan et al.[25] meets the conditions outlined in Theorem 2.1.2. The function proposed is

$$L(I, R) = \frac{I - I^*}{N} - \frac{I^*}{N} \ln \frac{I}{I^*} + \frac{\beta}{2\gamma N}(R - R^*)^2.$$

First note that we have

$$L(I^*, R^*) = I^*(1 - \ln e) + \frac{\beta}{2\gamma N} \cdot 0 = 0.$$

We note that $\frac{I}{I^*} - \ln e\frac{I}{I^*} > 0$ for $I \neq I^*$. Therefore, for $(I, R) \neq (I^*, R^*)$, we have

$$\begin{aligned} L(I, R) &= \frac{I^*}{N}\left( I - I^* \ln e\frac{I}{I^*} \right) + \frac{\beta}{2\gamma N}(R - R^*)^2 \\ &= \frac{I^*}{N} \underbrace{\left( \frac{I}{I^*} - \ln e\frac{I}{I^*} \right)}_{>0} + \frac{\beta}{2\gamma N}(R - R^*)^2 > 0. \end{aligned} \tag{2}$$

The final case to consider is when $I = I^*$ but $R \neq R^*$. In this case, we have

$$L(I^*, R) = \frac{\beta}{2\gamma N}(R - R^*)^2 > 0,$$

so $L$ is positive-definite. We also have that $L \to \infty$ whenever $I, R \to \infty$, so $L$ is radially unbounded. It is left to show that the time derivative of $L$ is negative-definite. O'Regan et al. reduce the dimension of the $SIRS$ system through the assumption of constant population and elimination of the susceptible class. System (1) becomes

$$\begin{aligned} I' &= -\mu I + \frac{\beta(N-I-R)I}{N} - \gamma I = \left(\beta - \frac{\beta I}{N} - \frac{\beta R}{N} - \gamma - \mu\right) I \\ R' &= -(\mu+\psi)R + \gamma I. \end{aligned} \tag{3}$$

Noting that, at the endemic equilibrium, we have

$$\frac{\beta(I^*+R^*)}{N} = \beta - \mu - \gamma \quad \text{and} \quad (\mu+\psi)R^* - \gamma I^* = 0,$$

we get the following simplified system:

$$\begin{aligned} I' &= I\left(\frac{\beta}{N}(I^*-I) + \frac{\beta}{N}(R^*-R)\right) \\ R' &= (\mu+\psi)(R^*-R) - \gamma(I^*-I). \end{aligned} \tag{4}$$

We will now verify that the time derivative of $L$ is negative-definite. We have

$$\begin{aligned} \frac{dL}{dt} &= \frac{\partial L}{\partial I}\cdot\frac{dI}{dt} + \frac{\partial L}{\partial R}\cdot\frac{dR}{dt} \\ &= (1-\frac{I^*}{I})I' + \frac{\beta}{\gamma N^2}(R-R^*)R' \\ &= (1-\frac{I^*}{I})I\left(\frac{\beta}{N}(I^*-I) + \frac{\beta}{N}(R^*-R)\right) + \frac{\beta}{\gamma N}(R-R^*)\left((\mu+\psi)(R^*-R) - \gamma(I^*-I)\right) \\ &= -\frac{\beta}{N}(I^*-I)^2 - \frac{\beta}{N}(I^*-I)(R^*-R) + \frac{\beta}{N}(I^*-I)(R^*-R) - \frac{\beta}{\gamma N}(\mu+\psi)(R-R^*)^2 \\ &= -\frac{\beta}{N^2}(I^*-I)^2 - \frac{\beta}{\gamma N^2}(\mu+\psi)(R-R^*)^2 < 0. \end{aligned} \tag{5}$$

Therefore $L$ is a Lyapunov function for the positive orthant, and consequently the endemic equilibrium is globally asymptotically stable.

□

It is important to note that the Lyapunov function provided in O'Regan et al. [25] did not meet the conditions for Lyapunov's second theorem (non-zero at equilibrium). The Lyapunov function used in O'Regan's model is given by

$$L(I, R) = I - I^* \ln I + \frac{\beta}{2\gamma}(R - R^*)^2 \tag{6}$$

$$L(I^*, R^*) = I^*(1 - \ln I^*) \neq 0. \tag{7}$$

A translation was made to ensure that the Lyapunov function was valid for system (1). This section serves as an introduction to the oscillatory nature of models with waning immunity and to justify the use of a simple Lyapunov function to determine stability of the disease-free equilibrium. In the following chapter, we will introduce a memory mechanism associated with the vaccination rate to demonstrate the ability to destabilize the endemic equilibrium and create persistent oscillations.

# Chapter 3

# Memory

The interplay between the spread of a disease such as influenza and individual vaccination decisions are quite complex. Not only do individuals base their vaccination decisions on their history of infection, influence of their peers or advice from medical professionals, they also base their decisions on past experience of infection and minor-to-severe vaccine complications [45]. These decisions are further confounded by mis-perceptions of disease severity, vaccine safety and experiences with influenza-like illnesses such as colds and "stomach flu". It is therefore inappropriate to restrict epidemic models of influenza to simple mass-action vaccination for voluntary vaccination campaigns. Several models have been proposed that address these issues using game theory and evolutionary game theory; however, we will restrict discussion of these methods for later chapters. Simply explained, a vaccination dilemma is created when individuals base their vaccination decisions on the current and/or past prevalence of infection. When disease prevalence is high, the risk of adverse effects from infection is greater, and vaccination is used for self-protection. In contrast, as a disease approaches an eradication threshold, the incentive to vaccinate is decreased. This dilemma is further exacerbated by an increase in perceived vaccination risk. A classic example of this is the drop in MMR (measles-mumps-rubella) vaccine coverage following dissemination of false information regarding false links between the MMR vaccine and autism, which has subsequently led to measles outbreaks in the United Kingdom [16] and at Disneyland in the US [15].

It has also been suggested that short-sighted vaccination behaviour may be responsible for erratic vaccination coverage for the flu in contact networks [9]. Although our model acts upon a well-mixed population, we obtain similar results. Essentially, by including a fading memory mechanism that counts the average prevalence of disease over a specified time period, we are able to construct a simplified free-riding dilemma without the need for game theory.

This chapter is organized as follows. First, a simple model that uses information-based vaccination is introduced and analyzed. Using the results of the previous chapter, global stability of the disease-free equilibrium will be shown, along with local asymptotic stability of the endemic equilibrium. A formal proof of conditions on the existence of a Hopf bifurcation are presented, and sensitivity analyses are conducted on available model outputs. Although we neglect other confounding effects, periodic dynamics are produced (such as those in presented in d'Onofrio et al.[28] and Eckalbar & Eckalbar [11]). This model will be later integrated into an evolutionary game theory model in Chapter 6.

## 3.1 Model assumptions and governing equations

The use of fading memory mechanisms have been previously studied in various contexts [27, 28, 31]. In this chapter, we propose a simple model in which individuals are vaccinated at a rate proportional to the prevalence of infection over a certain number of years, which decays at an exponential rate. This simple modification to the SIRV model is sufficient to sustain the dampening periodic oscillations of the original model. The model assumptions and equations are:

1. Individuals die at rate $\mu$ and are born at rate $\Lambda = N \cdot \mu$ to ensure an asymptotically constant population size.

2. Susceptible individuals ($S$) are infected at rate $\beta$ following contact with an infectious individual under the assumption of frequency-dependent contact and are moved to the infectious compartment ($I$).

3. Infected individuals ($I$) remain infectious for $\frac{1}{\gamma}$ days, recovering with immunity and are moved to the recovered class. We assume there is no disease-related mortality.

4. Recovered individuals maintain infection-induced immunity for $\frac{1}{\psi}$ days before immunity wanes and they are moved back to the susceptible compartment ($S$).

5. The average number of infections over $\theta$ seasons are counted ($M$) and are forgotten using an exponentially fading memory mechanism.

6. Susceptible individuals vaccinate at vaccination rate $\rho$ bilinearly to the number of susceptible individuals ($S$) and the memory of prevalence ($M$), moving to the vaccinated compartment ($V$).

7. Vaccinated individuals maintain vaccine-induced immunity for $\frac{1}{\phi}$ days before immunity wanes and they are moved back to the susceptible compartment ($S$).

The model is thus given by

$$\begin{aligned} S' &= \Lambda - \mu S - \frac{\beta SI}{N} - \rho SM + \psi R + \phi V \\ I' &= \frac{\beta SI}{N} - \mu I - \gamma I \\ R' &= \gamma I - \mu R - \psi R \\ V' &= \rho SM - \mu V - \phi V \\ M' &= \frac{\beta SI}{\theta N} - \eta M. \end{aligned} \tag{8}$$

For a description of all parameters, states and other notation, see Table 1.

## 3.2 Analysis

In this section, we will determine conditions on the existence of each equilibrium point as well as conditions on the local asymptotic stability of the endemic equilibrium and global asymptotic stability of the disease-free equilibrium using the results from

Chapter 2. We finish this section with a proof of a generalized Hopf bifurcation occurring for system (8).

**Proposition 3.2.1.** *The region* $\Gamma = \{(S, I, R, V, M) \in \mathbb{R}^5 | S, I, R, V, M \geq 0\}$ *is positively invariant under the flow of system* (8).

**Proposition 3.2.2.** *The disease-free equilibrium is given by*

$$X_0 = (S_0, I_0, R_0, V_0, M_0) = \left(\frac{\Lambda}{\mu}, 0, 0, 0, 0\right)$$

*and is globally asymptotically stable if* $\mathcal{R}_0 = \frac{\beta}{\gamma+\mu} < 1$*; otherwise, it is unstable.*

*Proof.* We will use the Lyapunov function $L = \frac{1}{2}I^2$ described in Chapter 2 to determine stability of the disease-free equilibrium. When we define $U = \{(S, I, R, V, M) \in \mathbb{R}^{5+}_0 | I = 0\}$, we have that $L$ is positive semi-definite with negative semi-definite time derivative in the sense of Theorem 2.1.4. Solutions eventually enter the region $\{(S, I, R, V, M) \in \mathbb{R}^{5+}_0 | S + I + R + V \leq \frac{\Lambda}{\mu}\}$ and never leave. These properties guarantee that solutions approach $U$ asymptotically. We will next show that solutions in $U$ converge asymptotically to the disease-free equilibrium. Once infection prevalence is null ($I = 0$), the memory function is strictly decreasing ($M' < 0$). It follows that $\lim_{t\to\infty} M = 0$. Substituting $I = M = 0$ into system (8), we also have that $R', V' < 0$, and it follows that $\lim_{t\to\infty} R = \lim_{t\to\infty} V = 0$ and $\lim_{t\to\infty} S = \lim_{t\to\infty} \frac{\Lambda}{\mu} - I - R - V = \frac{\Lambda}{\mu}$. Solutions beginning in $U$ therefore converge asymptotically to the disease-free equilibrium $X_0$. From the result of Theorem 2.1.4, $X_0$ is globally asymptotically stable. □

**Proposition 3.2.3.** *The endemic equilibrium is given by*

$$\begin{aligned}\bar{X} &= (\bar{S}, \bar{I}, \bar{R}, \bar{V}, \bar{M}) \\ &= \left(\frac{\Lambda(\mu+\gamma)}{\mu\beta}, \bar{I}, \frac{\gamma}{\mu+\psi}\bar{I}, \frac{\Lambda\rho(\mu+\gamma)^2}{\mu\beta\theta\eta(\mu+\phi)}\bar{I}, \frac{\mu+\gamma}{\theta\eta}\bar{I}\right)\end{aligned}$$

*where* $\bar{I} = \frac{\Lambda\theta\eta(\beta-\mu-\gamma)(\mu+\psi)(\mu+\phi)}{\mu\beta\theta\eta(\mu+\phi)(\mu+\psi+\gamma)+\Lambda\rho(\mu+\psi)(\mu+\gamma)^2}$ *and exists if and only if* $\mathcal{R}_0 = \frac{\beta}{\gamma+\mu} > 1$.

To simplify the analysis, we may make a few assumptions and alterations to the model to reduce the number of equations in system (8). First, we will assume that the rate at which infection-induced immunity wanes is the same as vaccine-induced immunity ($\phi = \psi$). This is not a large assumption to make, as individuals may be susceptible to a different strain in the following season. Next, we will consider that the recovered class includes any vaccinated or recovered individuals. Setting $R_V \equiv R+V$, we obtain the following system of equations:

$$\begin{aligned} S' &= \Lambda - \mu S - \frac{\beta SI}{N} - \rho SM + \psi R_V \\ I' &= -\mu I + \frac{\beta SI}{N} - \gamma I \\ R_V' &= -\mu R_V + \gamma I - \psi R_V + \rho SM \\ M' &= \frac{1}{\theta}\left(\frac{\beta SI}{N} - \theta\eta M\right). \end{aligned} \tag{9}$$

System (9) can be further simplified by assuming a constant population size ($R_V = N - S - I$). These simplifications reduce the burden of analysing the stability of the system by reducing it to three dimensions. Since systems (8) and (9) are roughly equivalent, the stability of the disease-free equilibrium is maintained. The simplified system is given by:

$$\begin{aligned} S' &= \Lambda - \mu S - \frac{\beta SI}{N} - \rho SM + \psi(N - S - I) \\ I' &= -\mu I + \frac{\beta SI}{N} - \gamma I \\ M' &= \frac{1}{\theta}\left(\frac{\beta SI}{N} - \theta\eta M\right). \end{aligned} \tag{10}$$

**Proposition 3.2.4.** *The disease-free equilibrium of system* (10) *is given by*

$$X^* = (S^*, I^*, M^*) = \left(\frac{\Lambda}{\mu}, 0, 0\right).$$

*$X^*$ is globally asymptotically stable whenever $\mathcal{R}_0 = \frac{\beta}{\mu+\gamma} < 1$; otherwise, it is unstable.*

**Proposition 3.2.5.** *The endemic equilibrium of system* (10) *is given by*

$$X_E = (S_E, I_E, M_E) = \left(\frac{\Lambda(\mu+\gamma)}{\mu\beta}, \frac{\Lambda(\beta-\mu-\gamma)\theta\eta(\mu+\psi)}{\mu\beta\theta\eta(\mu+\psi+\gamma) + \Lambda\rho(\mu+\gamma)^2}, \frac{\mu+\gamma}{\theta\eta}I_E\right)$$

*and exists if and only if* $\mathcal{R}_0 > 1$. *Furthermore, when it exists, the endemic equilibrium is locally asymptotically stable whenever the following condition is satisfied:*

$$\frac{a_1 a_2}{\eta(\beta-\mu-\gamma)(\mu+\psi)} > 1,$$

with

$$\begin{aligned} a_1 &= \frac{\eta(\beta-\mu-\gamma)(\mu+\psi)\left(2\Lambda\rho(\mu+\gamma)+\mu\beta\theta(\mu+\gamma+\psi+\eta)\right)}{\mu\beta\theta\eta(\mu+\psi+\gamma)+\Lambda\rho(\mu+\gamma)^2} + \eta(\mu+\psi) \\ a_2 &= \frac{(\beta-\mu-\gamma)(\mu+\psi)(\Lambda\rho(\mu+\gamma)+\mu\beta\theta\eta)}{\mu\beta\theta\eta(\mu+\psi+\gamma)+\Lambda\rho(\mu+\gamma)^2} + \mu+\psi+\eta. \end{aligned}$$

*Proof.* For the endemic equilibrium to exist, we must have $I_E > 0$. From the expression for $I_E$, we obtain directly that the endemic equilibrium exists if and only if $\beta-\gamma-\mu > 0$ or if $\mathcal{R}_0 = \frac{\beta}{\gamma+\mu} > 1$. Next, we will determine conditions on the stability of the endemic equilibrium. The Jacobian of system (10) is given by:

$$\begin{aligned} J(X_E-\lambda I) &= \begin{bmatrix} -\mu-\frac{\beta I_E}{N}-\rho M_E-\psi-\lambda & -\frac{\beta S_E}{N}-\psi & -\rho S_E \\ \frac{\beta I_E}{N} & -\mu+\frac{\beta S_E}{N}-\gamma-\lambda & 0 \\ \frac{\beta I_E}{\theta N} & \frac{\beta S_E}{\theta N} & -\eta-\lambda \end{bmatrix} \\ &= \begin{bmatrix} -\mu-\frac{\beta I_E}{N}-\rho M_E-\psi-\lambda & -\mu-\gamma-\psi & -\rho S_E \\ \frac{\beta I_E}{N} & -\lambda & 0 \\ \frac{\beta I_E}{\theta N} & \frac{\mu+\gamma}{\theta} & -\eta-\lambda \end{bmatrix}. \end{aligned} \tag{11}$$

The characteristic equation of the above Jacobian matrix is given by

$$\lambda^3 + a_2\lambda^2 + a_1\lambda + a_0 = 0.$$

where

$$\begin{aligned} a_0 &= \eta(\beta-\mu-\gamma)(\mu+\psi) \\ a_1 &= \frac{\eta(\beta-\mu-\gamma)(\mu+\psi)\left(2\Lambda\rho(\mu+\gamma)+\mu\beta\theta(\mu+\gamma+\psi+\eta)\right)}{\mu\beta\theta\eta(\mu+\psi+\gamma)+\Lambda\rho(\mu+\gamma)^2} + \eta(\mu+\psi) \\ a_2 &= \frac{(\beta-\mu-\gamma)(\mu+\psi)(\Lambda\rho(\mu+\gamma)+\mu\beta\theta\eta)}{\mu\beta\theta\eta(\mu+\psi+\gamma)+\Lambda\rho(\mu+\gamma)^2} + \mu+\psi+\eta. \end{aligned} \tag{12}$$

To determine stability of the endemic equilibrium, we proceed using the Routh–Hurwitz criteria for a cubic polynomial. For all eigenvalues to have negative real

part, it is required that $a_0, a_1, a_2 > 0$ and that $a_2 a_1 > a_0$. The first condition is satisfied for all coefficients as long as $\mathcal{R}_0 > 1$ (notably, whenever $\mathcal{R}_0 < 1$, we have $a_0 < 0$). Therefore the endemic equilibrium is unstable whenever $\mathcal{R}_0 < 1$. If instead $\mathcal{R}_0 > 1$, then there are no negative coefficients and we are able to state that the endemic equilibrium is locally asymptotically stable when $a_1 a_2 > a_0$ or

$$\frac{a_1 a_2}{\eta(\beta - \mu - \gamma)(\mu + \psi)} > 1.$$

as required. □

**Definition 3.2.6.** Consider a system of ordinary differential equations $\mathbf{x}' = \mathbf{F}(\mathbf{x}, \mu)$, $\mathbf{x} \in \mathbb{R}^{\mathbf{n}}$, $\mu \in \mathbb{R}$, with equilibrium point at $(\mathbf{x_0}, \mu_\mathbf{0})$. The system undergoes a Hopf bifurcation at $(\mathbf{x_0}, \mu_\mathbf{0})$ provided that:

1. The Jacobian $D_x\mathbf{F}|_{(\mathbf{x_0}, \mu_\mathbf{0})}$ has a pair of pure imaginary eigenvalues, and no other eigenvalues with zero real part.

2. The real part of the purely imaginary eigenvalues cross zero with non-zero speed; $\frac{d}{d\mu}[Re(\lambda(\mu)))|_{(\mu=\mu_0)} \neq 0$.

**Lemma 3.2.7.** *A cubic equation $x^3 + a_2 x^2 + a_1 x + a_0 = 0$ with positive coefficients has two purely imaginary roots if and only if $a_1 a_2 = a_0$.*

*Proof.* Let $x = \pm iz$ be the purely imaginary roots of the above cubic equation. Substituting these roots into the above equation gives

$$-iz^3 - a_2 z^2 + a_1 iz + a_0 = 0 \tag{13}$$

$$iz^3 - a_2 z^2 - a_1 iz + a_0 = 0. \tag{14}$$

Adding equation (13) to (14), we get $z^2 = \frac{a_0}{a_2}$, and subtracting equation (14) from (13), we obtain $z^2 = a_1$ or $z = 0$. The case where $z = 0$ implies that $a_0 = 0$ and consequently that $\mathcal{R}_0 = 1$, which is not considered for the proof of the Hopf bifurcation. Therefore we have that $a_1 a_2 = a_0$ as required.

Conversely, suppose $a_1 a_2 = a_0$. Then we have that

$$\begin{aligned} x^3 + a_2 x^2 + a_1 x + a_0 &= 0 \\ x^3 + a_2 x^2 + a_1 x + a_1 a_2 &= 0 \\ x^2(x + a_2) + a_1(x + a_2) &= 0 \\ (x^2 + a_1)(x + a_2) &= 0 \end{aligned}$$

The complex roots are therefore purely imaginary, with $x = \pm i\sqrt{a_1}$. □

**Theorem 3.2.8.** *System* (10) *undergoes a generalized Hopf bifurcation whenever* $a_1 a_2 = a_0$ *and*

$$\frac{\left[(\mu+\psi)(\delta\Delta_2+\omega)(\delta\Delta_1+\omega) + \alpha\mu\beta\omega\delta(\mu+\gamma+\psi) - \delta\omega^2\right]^2}{4\alpha\mu\beta\omega\delta(\mu+\psi)(\mu+\gamma+\psi)(\delta\Delta_2+\omega)\left(\delta\Delta_1+\omega\right)} > 1,$$

*where* $\delta = \beta - \mu - \gamma$, $\alpha = \theta\eta$, $\Delta_1 = \Lambda\rho(\mu+\gamma) + \mu\beta\theta\eta$, $\Delta_2 = 2\Lambda\rho(\mu+\gamma) + \mu\beta\theta\eta$ *and* $\omega = \mu\beta\theta\eta(\mu+\psi+\gamma) + \Lambda\rho(\mu+\gamma)^2$.

*Proof.* Both conditions of Definition 3.2.6 must be satisfied. As a consequence of Lemma 3.2.7, whenever $a_1 a_2 = a_0$, there are two purely imaginary eigenvalues $\lambda$ and $\bar{\lambda}$. It is sufficient for the second condition to show that $g \equiv a_1 a_2 - a_0$ crosses zero with non-zero speed for any parameter, since through Routh–Hurwitz conditions $\mathrm{sgn}(Re(\lambda)) = \mathrm{sgn}(a_1 a_2 - a_0)$. Although we will only demonstrate that a Hopf bifurcation occurs while varying $\theta$, it is also possible to obtain them through varying other parameters of the system. We have

$$g = \frac{A\theta^2 + B\theta + C}{\theta^2\phi},$$

where

$$\begin{aligned} A &= \alpha\delta(\mu+\gamma+\psi)(\mu+\psi)^2 \\ B &= (\mu+\psi)(\delta\Delta_2+\omega)(\delta\Delta_1+\omega) + \alpha\mu\beta\omega\delta(\mu+\gamma+\psi) - \delta\omega^2 \\ C &= \alpha^2\omega(\mu+\psi)(\delta\Delta_1+\omega). \end{aligned}$$

Since the numerator of $g$ is quadratic, $g$ has exactly one local extrema. Furthermore, when $g$ has exactly one root, the derivative of $g$ at the root is null. When

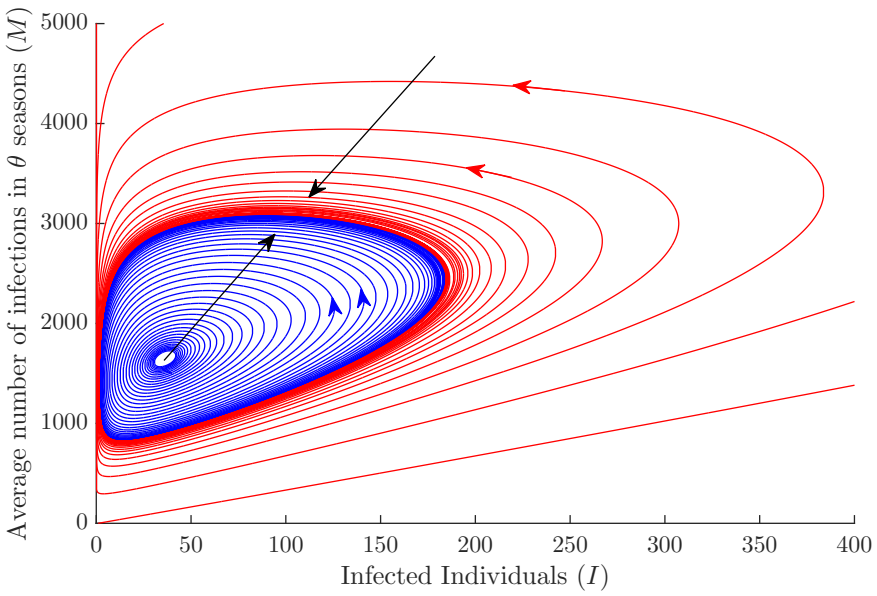


Figure 2: Time series of infected individuals versus average number of infections in $\theta$ seasons ($M$) for system (10) with $\mathcal{R}_0 > 1$, $a_1 a_2 > a_0$ and the conditions of Theorem 3.2.8 satisfied. Solutions oscillate and reach a stable limit cycle.

$g$ has two distinct real roots, then $g'$ is non-zero at these values. In other words, $a_1 a_2 - a_0$ crosses zero with non-zero speed whenever $B^2 - 4AC > 0$. Therefore a Hopf bifurcation occurs whenever $a_1 a_2 = a_0$ and

$$\frac{\left[(\mu+\psi)(\delta\Delta_2+\omega)(\delta\Delta_1+\omega)+\alpha\mu\beta\omega\delta(\mu+\gamma+\psi)-\delta\omega^2\right]^2}{4\alpha\mu\beta\omega\delta(\mu+\psi)(\mu+\gamma+\psi)(\delta\Delta_2+\omega)\left(\delta\Delta_1+\omega\right)} > 1.$$

□

We would like to note that the above result was obtained independently, although a similar proof was later found in [28].

## 3.3 Numerical Simulations

All numerical simulations and figures generated were completed in Matlab using the Runge–Kutta(4,5) method. Default absolute and relative integration error tolerances

Table 2: Parameter values used for numerical simulations of system (8). Parameter values in this table are used for all simulations in this section unless otherwise stated.

| Parameter | Description | Simulation value | Ref. |
|---|---|---|---|
| $\mu$ | Human death rate | $\frac{1}{80 \cdot 365}$ | [46] |
| $\Lambda$ | Human birth rate | $10000\mu$ | Calculated |
| $\beta$ | Contact rate | 0.3 | [a] |
| $\gamma$ | Recovery rate | $\frac{1}{8}$ | [7] |
| $\psi$ | Rate of waning immunity (natural) | $\frac{1}{150}$ | [8][b] |
| $\phi$ | Rate of waning immunity (vaccine) | $\frac{1}{150}$ | [8][b] |
| $\rho$ | Vaccination rate | 0.00001 | Assumed[c] |
| $\theta$ | Memory span (seasons) | Varied | |

[a] Contact rate was chosen to give values of $\mathcal{R}_0 \in (1, 2.5)$.

[b] Rate of waning immunity (vaccine and naturally induced) were chosen to be equal and last for five months corresponding to a month before and after peak activity.

[c] Vaccination rate was chosen to allow for periodic dynamics.

were too large to ensure solutions remained non-negative as they approached the boundary of the positive orthant and were changed to $10^{-12}$ to ensure they remained non-negative. Parameter values for the simulations of this chapter are provided in Table 2 unless otherwise specified. A more thorough discussion on the choice of parameter values is given in Chapter 5. Results of the simulations for long lengths of memory span produce similar behaviour to those of a classic $SIR$ model with vaccination (results shown in Figure 3). However, by altering the vaccination rate and reducing the length of memory sufficiently, we were able to produce periodic dynamics. These results do not suggest that a simple memory mechanism alone is sufficient to create periodic dynamics with proper parameter values but serve to illustrate the results of Theorem 3.2.8 (shown in Figure 4).

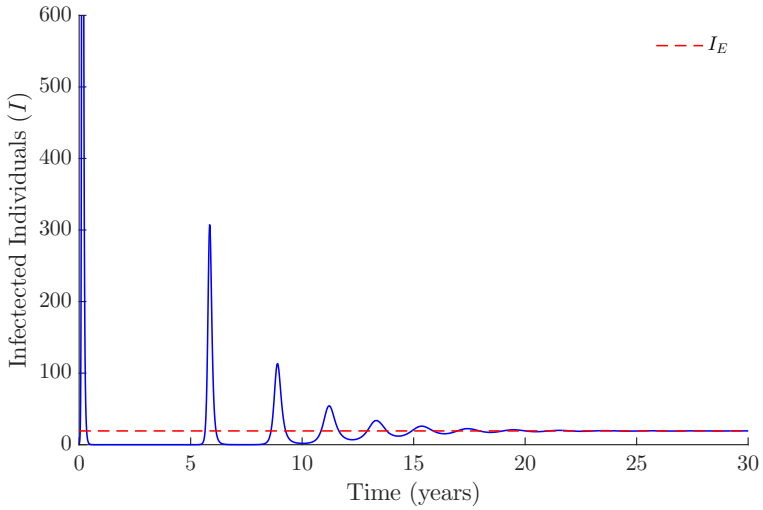


Figure 3: Time series of infected individuals for system (9) with $\mathcal{R}_0 > 1$ and $a_1 a_2 > a_0$ ($\theta = 2$) . Solutions oscillate and converge to the endemic equilibrium $X_E$. Initial conditions are set to $[N, N-1, 0, 0]$ where $N = 10000$. Other parameter values are chosen according to Table 2

.

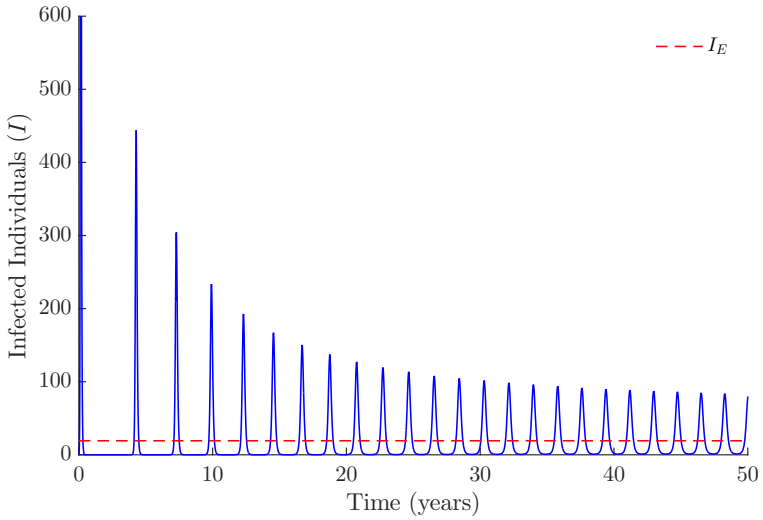


Figure 4: Time series of infected individuals for system (9) with $\mathcal{R}_0 > 1$, $a_1 a_2 < a_0$ and the conditions of Theorem 3.2.8 satisfied ($\theta = 0.3$) . Solutions oscillate and remain positive for all time. Initial conditions are set to $[N, N-1, 0, 0]$ where $N = 10000$. Other parameter values are chosen according to Table 2.

### 3.3.1 Sensitivity Analysis

In order to determine whether the parameters of our models are sensitive within the parameter ranges of interest, we will use the method of partial rank correlation coefficients (PRCCs) and Latin Hypercube Sampling (LHS). The expression for $\mathcal{R}_0$ is often used as the output for sensitivity analyses; however, the simple nature of $\mathcal{R}_0$ in all models studied exclude most of the model parameters. To circumvent this, the output for the sensitivity analyses will be chosen as endemic equilibrium points and/or any bifurcation or stability parameters.

To determine which parameters have a significant effect on the selected outputs, a set of $N = 1000$ sample parameter sets are analyzed using PRCCs, following the method of Blower and Dowlatabadi [6]. The parameter sets were chosen using LHS originally developed by Mckay [20]. In this method, a range is chosen for each parameter and is subsequently divided into $N$ equal intervals. This creates a hypercube with $N^k$ cells, where $k$ is the number of parameters in the sample. For each input

parameter, a single value is chosen randomly from each interval under a uniform distribution in such a way that, in each sample generated, no parameter is sampled from the same interval more than once. For example, for a first sample, a value for the contact rate $\beta$ is chosen from the thirteenth interval; therefore no other sample can use a value of $\beta$ from the thirteenth interval. A simple way to illustrate this is to place $N$ rooks on an $N \times N$ chessboard in such a way that no rook can take out another (noting that rooks can only move in straight lines and are not permitted to move diagonally). The analogy can be extended to higher dimensions by adding new available directions (always moving in straight lines). Once generated, each sample was used to calculate the value of their respective output parameter. The number of infected individuals at the endemic equilibrium ($I_E$) of system (10) was used as the output parameter in Figures 5 and 6, whereas one of the bifurcation parameters ($\frac{a_1 a_2}{a_0}$) was used for Figures 7 and 8. PRRCs were then used to determine the sensitivity of these outputs. The results are shown in the above-mentioned figures.

Model parameters and ranges were determined when available from the literature or were estimated. The contagious period of influenza may begin up to a day before symptoms develop and up to five to seven days after onset of symptoms [7]. We therefore chose a range for the recovery rate between $\frac{1}{8}$ and $\frac{1}{4}$. Since values of the endemic equilibrium become negative when $\mathcal{R}_0 < 1$, values for the contact rate were chosen to give values of $\mathcal{R}_0 > 1$. The length of infection and vaccine-induced immunity were chosen to protect individuals for the length of the flu season (approximately five months [7]). Longer periods of immunity such as one year would allow for individuals to be protected by infection or vaccine-induced immunity in the following season, which may not occur due to new circulating strains in the following season. Ranges were therefore chosen between $\frac{1}{200}$ and $\frac{1}{100}$ for both waning-immunity parameters. The length of memory was given a broad range due to the lack of concrete data on individuals' memory of past infection. Finally, the same vaccination rate as the simulations was used (scaled according to population size) with the range with an order of magnitude above and below for the parameter range. The ranges are summarized in Table 3.

Figure 5 shows that the number of infected individuals at the endemic equilibrium

Table 3: Minimum and maximum values for PRCC/LHS using uniform distribution for system (10).

| **Figures 5-6** | | | **Figures 7-8** | | |
|---|---|---|---|---|---|
| Parameter | Minimum | Maximum | Parameter | Minimum | Maximum |
| $\mu$ | $\frac{1}{90\cdot365}$ | $\frac{1}{70\cdot365}$ | $\mu$ | $\frac{1}{90\cdot365}$ | $\frac{1}{70\cdot365}$ |
| $\beta$ | 0.25 | 0.6 | $\beta$ | 0.25 | 0.6 |
| $\gamma$ | $\frac{1}{8}$ | $\frac{1}{4}$ | $\gamma$ | $\frac{1}{8}$ | $\frac{1}{4}$ |
| $\phi$ | $\frac{1}{200}$ | $\frac{1}{100}$ | $\psi$ | $\frac{1}{200}$ | $\frac{1}{100}$ |
| $\psi$ | $\frac{1}{200}$ | $\frac{1}{100}$ | $\theta$ | 0.1 | 4 |
| $\theta$ | 0.1 | 4 | $\rho$ | $\frac{0.01}{N}$ | $\frac{0.6}{N}$ |
| $\rho$ | $\frac{0.01}{N}$ | $\frac{0.6}{N}$ | | | |

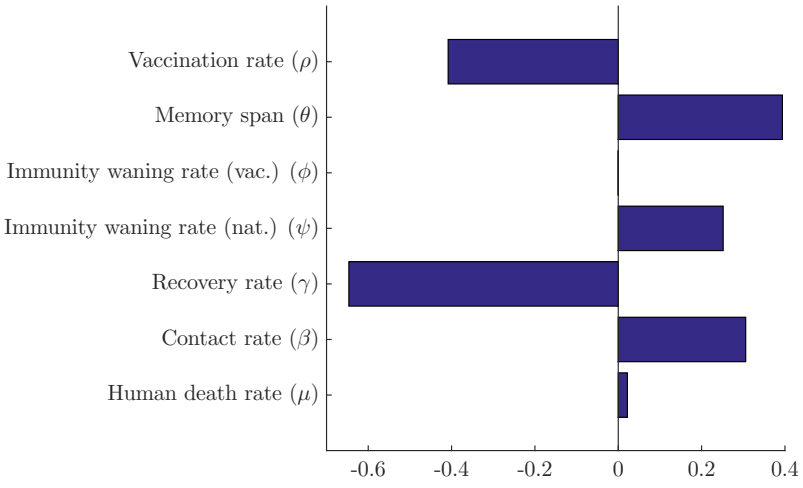


Figure 5: PRCC sensitivity analysis with $N = 1000$ simulations for listed parameters of system (10) using ranges from Table 3 and the number of infected individuals at the endemic equilibrium ($I_E$) as the output.

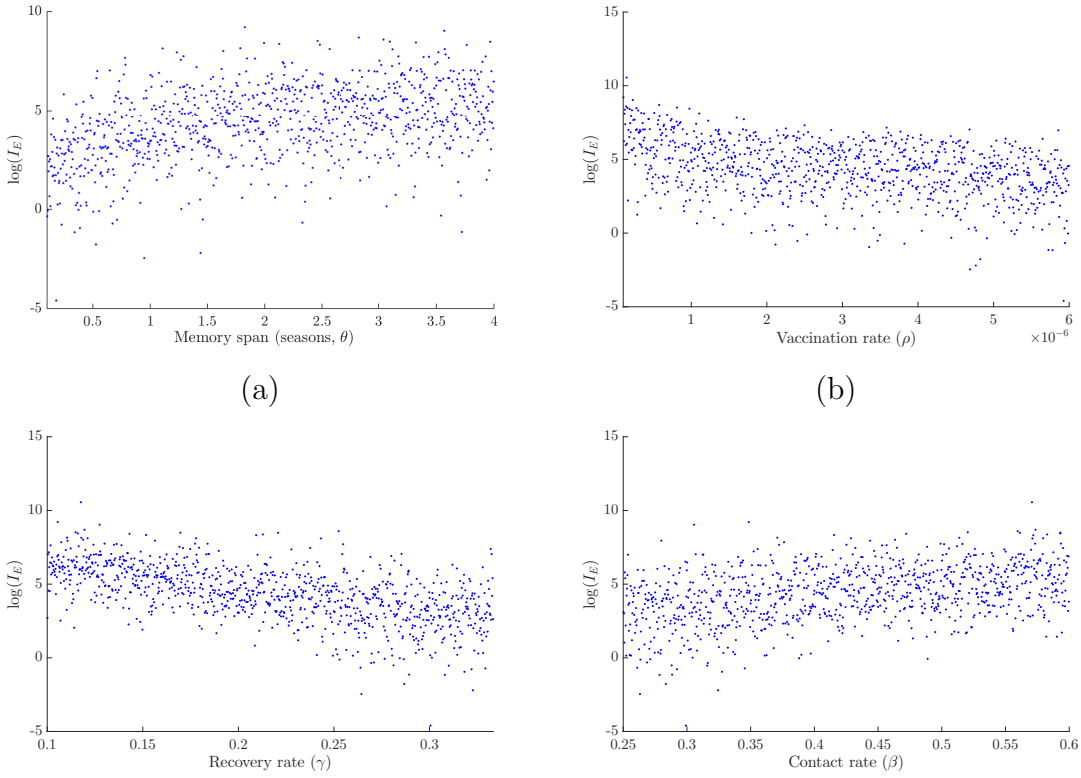


Figure 6: Dependence of $I_E$ on the four most sensitive parameters (determined from the PRCCs) of system (10): (a) length of memory span ($\theta$), (b) vaccination rate ($\rho$), (c) recovery rate ($\gamma$) and (d) the contact rate ($\beta$). Results were generated over $N = 1000$ simulations with parameter ranges shown in Table 3.

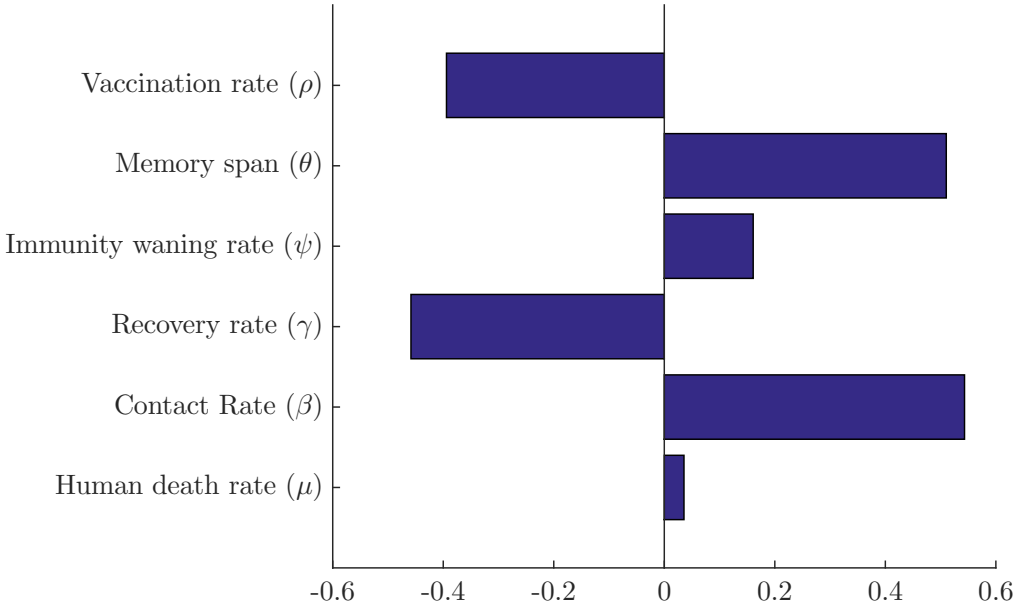


Figure 7: PRCC sensitivity analysis with $N = 1000$ simulations for listed parameters of system (10) using ranges from Table 3 and the stability parameter of the endemic equilibrium $\left(\frac{a_1 a_2}{a_0}\right)$ as the output.

$(I_E)$ is most sensitive to the recovery rate. This was expected, as individuals are able to infect more individuals as the length of the contagious period is increased. The endemic equilibrium was also expected to be sensitive to the length of memory as well as the vaccination rate. The bifurcation parameter $\left(\frac{a_1 a_2}{a_0}\right)$ was most sensitive to the contact rate, the memory span and the recovery rate (shown in Figure 7). The sensitivity to the length of memory was expected, as a large range was chosen. The corresponding Monte Carlo outputs are provided in Figures 6 and 8. In Figure 8, points lying above the red line correspond to a locally asymptotically stable endemic equilibrium, while points lying below this line indicate the potential for periodic solutions.

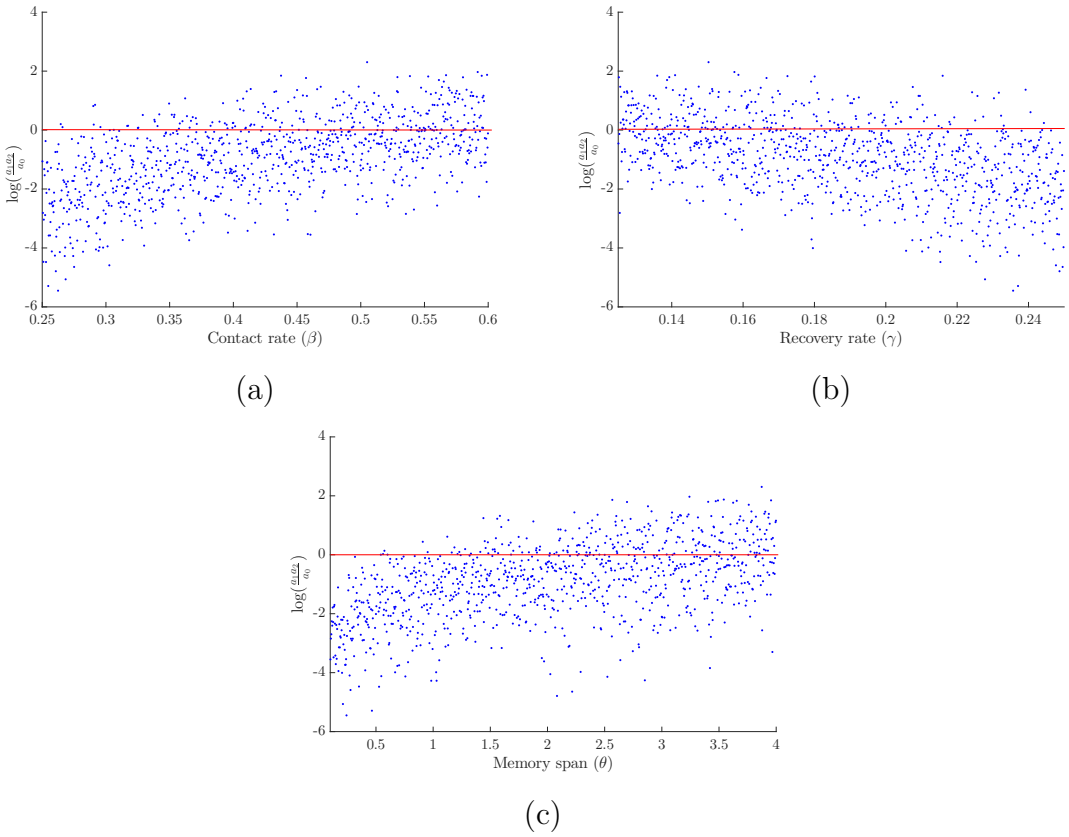


(a) (b)

(c)

Figure 8: Dependence of the bifurcation parameter $\left(\frac{a_1 a_2}{a_0}\right)$ on the three most sensitive parameters (determined from the PRCCs) of system (10): (a) contact rate ($\beta$), (b) recovery rate ($\gamma$), and (c) the memory span ($\theta$). Results were generated over $N = 1000$ simulations with parameter ranges shown in Table 3. Points above the red line represent a simulation with a locally asymptotically stable endemic equilibrium, while points below represent potential for periodic solutions.

## 3.4 Discussion

By using a model in which individuals choose to vaccinate based solely on their memory of past infection, complicated dynamics may occur. When individuals have short-sighted vaccination behaviour, periodic dynamics may be observed through a Hopf bifurcation. Generally, SIRVS models do not exhibit such periodic dynamics without seasonal forcing. Although it has been shown that there is a positive correlation between individuals seeking vaccination and a recent infection, the length of memory needed to create periodic dynamics in this model is less than one year. This short length of memory is unrealistic; however, it does show how a relatively simple epidemic model may be destabilized through the effects of personal experience with the disease. It also shows why it is important to model the effects of human behaviour when studying vaccination as a method of reducing the burden of vaccine-preventable diseases such as influenza.

The results of this model also demonstrate the dilemma posed by voluntary vaccination programs. As the disease prevalence begins to drop near eradication levels, individuals reduce vaccination rates, which creates a large enough pool of susceptible individuals to allow for subsequent outbreaks. The dilemma created by voluntary vaccination has been extensively studied [1, 2, 3, 4, 13, 24, 27, 28, 31, 45, 48]. Although our model requires individuals to have a very short memory span in regards to past infections, we will use this memory mechanism for models in later chapters, which will allow for similar results with longer memory spans.

This model also disregards effects such as the perceived risk of infection, the willingness to adopt vaccination, peer-influence and vaccine-associated risks. It is therefore not a full study of the effects of human vaccination behaviour but provides a simple introduction to the complex dynamics involved when these effects are included. The decaying memory model will be re-introduced with an evolutionary game-theoretic model in Chapter 6.

# Chapter 4

# Game Theory

Game theory is a field of mathematics pioneered by John Nash [23]. Essentially, game theory consists of determining the optimal strategy in a non-cooperative game with two or more players. Originally used in economics, game theory has since developed and been used many fields including population biology, ecology and epidemiology. By defining the expected payoffs for each strategy, a strategy can be found such that, no player can increase their payoff by switching strategies. This strategy is named the Nash equilibrium and is defined formally in Definition 4.0.1.

**Definition 4.0.1.** Let $(S, E)$ be a game with $n \geq 2$ players, where $S = S_1 \times S_2 \times \cdots \times S_n$ are the strategies of each player and $E_i(x)$, the corresponding payoff to player $i$ for a given strategy set $x \in S$. A strategy set $x^* = (x_1^*, x_2^*, \cdots, x_n^*)$ is a Nash equilibrium if for all players, no change in strategy is profitable to that player. Formally, let us define $\bar{x}_i^*$ as the Nash strategy $x^*$, less the strategy of player $i$ and $E_i(x_i, \bar{x}_i^*)$, as the payoff to player $i$ playing strategy $x_i \in S_i$ while the remaining players play according to $x^*$. Therefore, $x^*$ is a Nash equilibrium if $\forall i$, and all alternate strategies available to player $i$ ($x_i \in S_i$), we have that

$$E_i(x_i^*, \bar{x}_i^*) \geq E_i(x_i, \bar{x}_i^*).$$

As was shown in the previous chapter, simple human behaviour models can lead to complex dynamics. To include the effects that were neglected in the previous chapter such as the perceived risk of infection and vaccination, we introduce a game-theoretic

model. Game theory is well-suited for modeling human vaccination behaviour and there has been an increased interest in its extension from economics to ecology and epidemiology. Game theory has been used to study vaccine adherence in a broad sense, with applications to several childhood diseases [3, 4, 12, 13].

Classical deterministic models consist of individuals who act according to the flow of differential equations governing their movement. Whether or not an individual wishes to be vaccinated is not considered, and human behaviour is therefore neglected. These models do not allow for a detailed analysis of the free-riding dilemma that occurs in voluntary vaccination campaigns. Studies have frequently shown that self-interest in voluntary vaccination leads to sub-optimal vaccination coverage [3, 4, 13, 38]. This suggests that including individuals' rational behaviour is important when building epidemic models where the choice of self-protection through adoption of hygienic practices, social distancing and/or the use of vaccines is made at the individual level. In the following sections, we will adopt and alter a game-theoretic framework from the works of Bauch in order to analyze vaccination behaviour for influenza.

## 4.1 The epidemiological model

In this section, we explore the method used by Bauch and Earn [3] to determine the Nash equilibrium in terms of vaccination behaviour. Although used for smallpox, which is qualitatively different from influenza, we modified the classic model for influenza to adapt to the method proposed. Simplified transmission of influenza is classically modeled using an $SEIR$ model; however, this model is simply a rescaled version of the $SIR$ model. For simplicity, we will use an $SIR$ model similar to Bauch and Earn. The other fundamental difference between the models for smallpox and influenza is the age at vaccination. For smallpox, a proportion $p$ are vaccinated once they enter the population and move directly to the recovered class. The remaining proportion of individuals remain susceptible to the disease. Thus, individuals are vaccinated at the time they enter the population, making the time of vaccination at birth. This differs from influenza, where we vaccinate individuals at most ages with

a certain emphasis on those of increased risk such as seniors or individuals suffering from immunodeficiency diseases. The model proposed for smallpox is therefore incompatible with the method of vaccinating for influenza (unless a long-lasting universal vaccine became available). Many models use constant or linear vaccination terms in systems of ODEs; however, these methods increase the difficulty in analyzing vaccination behaviour using game theory. Instead, we propose the following modified $SIR$ model to circumvent these difficulties.

Instead of vaccinating a proportion of individuals as they enter the population, or by removing them to a vaccination/removed class, we will identify at the moment they get "infected". A successful infectious contact in a classic $SIR$ model will move an individual from the susceptible class to the infected class. In this modified model, once an individual has a successful infectious contact, they will either be moved to the recovered class with probability $p$, representing the coverage of vaccination in the population, or be moved classically to the infectious class. Due to the nature of mass-action models, this separation at the time of successful infectious contact diminishes the number of individuals becoming infected. This can easily be circumvented by rescaling the contact rate to maintain the shape of the epidemic curve. This mode of vaccination was chosen to limit the number of individuals who can receive vaccination. A critical assumption of this model is that individuals will have decided their vaccination status before the epidemic and receive complete protection from infection and have an infinitely fast recovery rate. The system of differential equations resulting from this modified model is given by system (15) with the following model assumptions:

1. Individuals die at rate $\mu$ are born into the system at rate $\Lambda = N\mu$ to ensure asymptotically constant population size.

2. Infected individuals ($I$) infect susceptible individuals (moving them to the $I$ compartment) at rate $\beta$, according to frequency-dependent transmission and with probability $(1 - p)$, corresponding the proportion of individuals who are not vaccinated in the population. If there is a successful contact between an infected individual and a vaccinated individual (probability $p$), the susceptible

individual does not get infected and moves directly to the recovered class ($R$).

3. Infected individuals remain infectious for a period of $\frac{1}{\gamma}$ days before recovering and moving to the recovered class ($R$).

4. Recovered individuals ($R$) remain immune to infection for all time.

$$\begin{aligned} S' &= \Lambda - \mu S - \frac{\beta SI}{N} \\ I' &= (1-p)\frac{\beta SI}{N} - \mu I - \gamma I \\ R' &= p\frac{\beta SI}{N} + \gamma I - \mu R. \end{aligned} \tag{15}$$

The disease-free equilibrium is given by $X_0 = \left(\frac{\Lambda}{\mu}, 0, 0\right)$. To find the value of $R_0$, we can directly determine the number of secondary infections from one infectious individual. In this model, once an individual is infectious, they leave the class at recovery rate $\gamma$, or die at rate $\mu$. Therefore, the average time spent in the infectious class is $\frac{1}{\gamma+\mu}$. While in the infectious class, susceptible individuals are infected at rate $\beta$, and those individuals are moved into the infected class with probability $(1-p)$. The number of secondary infections resulting from a single infected individual is therefore $R_0 = \frac{(1-p)\beta}{\gamma+\mu}$. Note that $R_0$ differs from $\mathcal{R}_0 = \frac{\beta}{\mu+\gamma}$. This value is also determined by analyzing the Jacobian matrix of the linearized system about the disease-free equilibrium, or by analyzing the values for which $I' < 0$, while $I \neq 0$. To determine the critical vaccination threshold, we set $R_0 = 1$ and solve for $p$ giving $p_{crit} = 1 - \frac{\gamma+\mu}{\beta}$. This is a minor difference from the model for smallpox, since it is not directly a function of $R_0$. When we decrease $p < p_{crit}$, we will see existence of the endemic equilibrium. Through some algebraic manipulations, we can determine the value of the endemic equilibrium.

$$X_E = (S_E, I_E, R_E) = \left(\frac{\Lambda}{\mu\mathcal{R}_0}, \frac{\Lambda(\mathcal{R}_0 - 1)}{\beta}, \frac{\Lambda(\beta - \mu\mathcal{R}_0)(\mathcal{R}_0 - 1)}{\mu\beta\mathcal{R}_0}\right),$$

where $\mathcal{R}_0 = \frac{\beta}{\gamma+\mu}$.

This model allows us to determine a key value necessary in calculating the Nash equilibrium: the probability of infection. Determining an algebraic definition for the

probability of infection is very difficult for relatively simple models and when it can be determined, has a very limited use. Following the method presented in Bauch and Earn [3], the probability of infection is defined as being the probability of a susceptible individual becoming infected versus dying per unit time. This definition lacks flexibility because it relies on the values of endemic equilibria, more accurately representing the probability of infection once the system reaches a stable state. For system (15), the probability of infection ($\pi_p$) of a susceptible individual in a population vaccinating with probability $p$, is given by

$$\pi_p = \frac{(1-p)\beta S_E I_E}{(1-p)\beta S_E I_E + \mu S_E} = \frac{(1-p)(R_0 - 1)}{R_0(1-p) + p}.$$

Although mass-action vaccination is traditionally used for epidemic models, we found that the probability of infection of a model with mass-action vaccination did not accurately represent reality. This is due to the fact that mass-action vaccination models do not allow for individuals to turn down vaccination indefinitely. As a simplified example, in the absence of disease in such a model, eventually all individuals become vaccinated regardless of the proportion who chose not to vaccinate. By allowing the vaccination status of an individual to be revealed at the point of infection, we can control a strict proportion $p$ of vaccinators.

## 4.2 Game-theoretic model

With the dynamics defined by the equations in (15), we are now able to define the vaccination game for influenza. Considering all individuals are playing with self-interest, without the effects of altruism, we define the payoff function for an individual who vaccinates with probability $P$, in a population where a proportion $p$ are vaccinated as

$$E(P, p) = P(-r_v) + (1 - P)(-r_i \pi_p),$$

where $r_v$ and $r_i$ denote the risk of vaccination and infection, respectively. In the context of a disease which may not be risky for some of the population, where a proportion of the population may perceive the vaccine to be risky, it is simpler to use

a term for relative risk $r = \frac{r_v}{r_i}$ by rescaling the payoff function to become

$$E(P, p) = -rP + (1 - P)\pi_p.$$

In a population where a proportion $\epsilon$ vaccinate with probability $P$ and a proportion $(1 - \epsilon)$ vaccinate with probability $Q$, the payoff functions become

$$E_P(P, Q, \epsilon) = E(P, \epsilon P + (1 - \epsilon)Q)$$
$$E_Q(P, Q, \epsilon) = E(Q, \epsilon P + (1 - \epsilon)Q).$$

This leads to the definition of the payoff gain function $\Delta E$, as the gain (or loss) received by an individual switching from the strategy of vaccinating with probability $Q$ to $P$

$$\Delta E = E_P - E_Q = [\pi_{P_T} - r](P - Q),$$

where $P_T = \epsilon P + (1 - \epsilon)Q$. The Nash equilibrium corresponds to the mixed strategy $(P \neq 0, P \neq 1)$, where no individual can increase their payoff by switching to another strategy. Since we will be assuming $P \neq Q$, we must have

$$\pi_{P^*} = r.$$

Substituting for the value of $\pi_p$ determined in the last section, we obtain the following second degree equation:

$$P^{*2}(R_0^*(r - 1) - P^*(2R_0^* - 1)(r - 1) + R_0^*(r - 1) + 1 = 0. \tag{16}$$

The solution to the above equation represents the Nash equilibrium of system (15). A detailed proof of the convergent stability of this equilibrium is provided in Bauch [3]. In Figure 9, we show the relation between the relative risk of vaccination with the probability of infection and the Nash equilibrium $P^*$. In contrast to Bauch and Earn's model, the probability of infection and the Nash equilibrium decrease faster as the relative risk increases; however, the results remain similar for low values of $\mathcal{R}_0$.

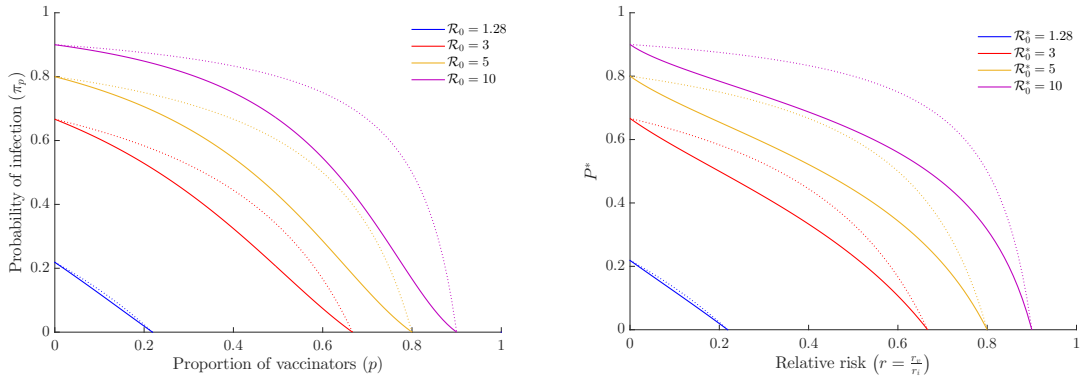


(a) (b)

Figure 9: (a) The probability of infection as a function of the proportion $p$ of vaccinators for varied values of $\mathcal{R}_0$. (b) The Nash equilibrium value of the proportion of vaccinators as a function of the relative risk of vaccination for varied values of $\mathcal{R}_0$. Dotted lines represent the results of Bauch and Earn [3] for vaccination at birth.

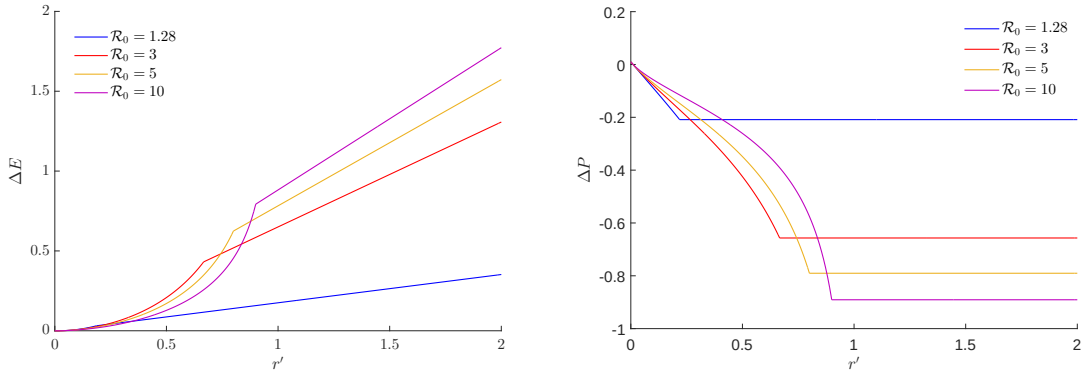


(a) (b)

Figure 10: (a) The payoff gain and (b) the change in vaccine uptake of an individual switching to the new convergently stable Nash equilibrium $P'$, with associated relative risk $r'$, following a vaccine scare while the remainder of the population continues to vaccinate according to the relative risk $r = 0.01$.

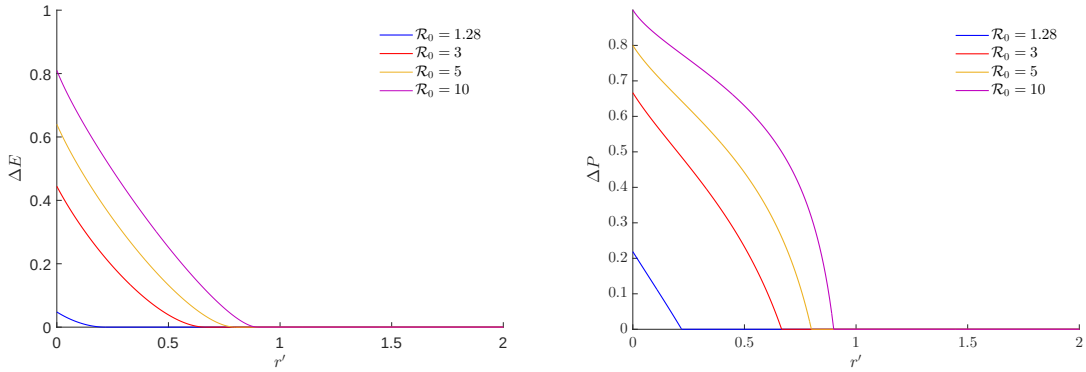


(a) (b)

Figure 11: (a) The payoff gain and (b) the change in vaccine uptake of an individual switching to the new convergently stable Nash equilibrium $P'$, with associated relative risk $r'$, following a vaccine education campaign while the remainder of the population continues to vaccinate according to the relative risk $r = 0.95$.

## 4.3 Numerical simulations

Following the analysis set out by Bauch and Earn, we will study the effects of a vaccine-scare on the population. It is assumed that individuals who do not seek vaccination consider the vaccine to be riskier than infection in absence of vaccination ($r > \pi_0$). In Figure 10, we consider a population which vaccinates according to the Nash equilibrium $P$, with associated risk $r = 0.01 < \pi_0$. We then calculate the perceived payoff gain of switching to the Nash equilibrium for a single individual, corresponding to a new relative risk $r' < r$ (Figure 10a). In the same way, we illustrate the drop in vaccine uptake for the individual in the same scenario (Figure 10b).

In Figure 11, we begin with a population with perceived relative-risk of vaccination $r = 0.95$ (to ensure that $r > \pi_0$ for all values of $\mathcal{R}_0$ studied) and show the payoff gain and the increase in vaccine uptake for an individual choosing to switch to vaccinating according to the new Nash equilibrium $P'$, with associated relative risk $r'$. The curves in Figures 10 and 11 are qualitatively similar to those in Bauch and Earn[3].

Sensitivity analyses on system (15) were conducted with the same ranges as were used in the previous chapter (see Table 3) using the solution of equation (16). A

Table 4: Parameter values and descriptions used for numerical simulations of system (15) and game-theoretic equations derived in Section 4.3. Parameter values in this table are used for all simulations unless otherwise stated.

| Parameter | Description | Simulation value | Ref. |
|---|---|---|---|
| $\mu$ | Human death rate | $\frac{1}{80 \cdot 365}$ | [46] |
| $\Lambda$ | Human birth rate | $10000\mu$ | Calculated |
| $\beta$ | Contact rate | 0.3 | Assumed[a] |
| $\gamma$ | Recovery rate | $\frac{1}{8}$ | [7] |
| $p$ | Proportion of vaccinating individuals | Varied | Assumed |
| $\pi_p$ | Probability of infection versus dying | | |
| $r_i$ | Scaled risk of infection | | |
| $r_v$ | Scaled vaccination risk | | |

[a] Contact rate was chosen to give values of $\mathcal{R}_0 \in (1, 2.5)$.

maximum bound for the relative risk of infection being only three times riskier than vaccination (much lower than expected) and a lower bound several orders of magnitude smaller, we found that the Nash equilibrium was not sensitive to the relative risk (graphs of results omitted).

## 4.4 Discussion

Following the same analysis from [3] of the payoff gain and change in vaccine uptake at the beginning and end of a vaccine scare, we obtain similar results. It takes longer to increase vaccination coverage after a vaccine scare than it does for it to decrease at the beginning of a scare. This becomes more important as the value of $\mathcal{R}_0$ decreases

closer to unity. For seasonal influenza, the median value of the basic reproductive ratio is $\mathcal{R}_0 \approx 1.28$ [5], which leads to low coverage levels at the convergently stable Nash equilibrium and a very small incentive to switch to a vaccination behaviour. It is assumed that for individuals who perceive the influenza vaccine as riskier than infection, that $r > \pi_0$ (where $\pi_0$ is the probability of infection without vaccination). Education programs aimed at these individuals must therefore successfully decrease the perceived risk of vaccination to much lower levels for the individual to perceive any personal benefit. For diseases with higher values of $\mathcal{R}_0$, the task of education becomes simpler. Assuming the Canadian population vaccinates according to the convergently stable Nash equilibrium, the perceived value of $\mathcal{R}_0 \approx 2.4$. This corroborates the results of surveys by Galvani [13] which show that individuals over-estimate the probability of influenza infection. As a result of the game-theoretic model, this perceived value of $\mathcal{R}_0$ is too low for there to be a significant payoff by switching to a vaccinator strategy from a non-vaccinator strategy. The change in vaccine uptake is also minimal, as the risk of infection decreases after a vaccine-scare for low values of $\mathcal{R}_0$. This suggests that for diseases with low $\mathcal{R}_0$, with low-risk vaccines such as with influenza, that there is not a significant effect from small increases or decreases in the perceived risk of vaccination. This further suggests that education campaigns for influenza vaccine safety, aimed towards individuals with high perceived relative risk, would lead to marginal increases in vaccine uptake.

The game theory presented in this chapter serves as an introduction to the use of payoff functions for evaluating risk. Although the game-theoretic model and the epidemic model both feed off each other to reach equilibrium, this feedback is limited. Individuals make their vaccination decision regardless of the current threat of infection and the probability of infection is calculated when the epidemic model is at equilibrium. The probability of infection is therefore not an appropriate measure throughout the influenza season. This model also assumes perfectly rational behaviour from all individuals and assumes that each individual has full knowledge of their probability of infection, as well as the costs of each potential outcome. Another issue that arises when implementing these models is the assumption that the probability of incurring cost due to infection is constant. For influenza, the probability of infection varies

greatly depending on the time of year and severity of the outbreak; individuals do not seek vaccination between influenza seasons and some seasons are worse than others. Although static game theory may not accurately represent the dynamics of a seasonal disease such as influenza, it serves to demonstrate the free-rider dilemma observed in society and the difficulties that public-health officers face when dealing with voluntary vaccination programs, vaccination scares and education programs. In the following chapter, we will introduce the notion of a dynamic game through Evolutionary Game Theory. These models will allow for individuals to switch behaviour in response to changing prevalence of infection among the population. These models better describe human behaviour in regards to vaccination and allow to better study the free-riding dilemma posed by voluntary vaccination campaigns.

# Chapter 5

# Evolutionary Game Theory

Evolutionary game theory was developed by John Maynard Smith and George R. Price [39] after the works of MacArthur and Hamilton on evolution of the sex ratio. Smith and Price wanted to understand why species evolved inefficient behaviours for intra-species competition such as the way male snake species wrestle each other but refuse to use their fangs. Classical game theory was not sufficient to describe this behaviour as animals do not choose these behaviours, they inherit them from their parents. The extension of game theory was the introduction of a lack of rationality in the players of the game; players are not necessarily choosing the Nash equilibrium as their strategy. Instead, individuals are playing some available strategy dependent on the distribution of strategies which is evolving over a large number of games played. This motivated Smith and Price to search for a strategy that would be stable under the effects of natural selection: an Evolutionary Stable Strategy.

**Definition 5.0.1.** An **Evolutionary Stable Strategy (ESS)** is a strategy such that if most of the population were to adopt it, any new strategy (first found at low incidence) would not provide a higher reproductive fitness. Formally, let $E_J(I)$ be the expected payoff of $I$ played against $J$. $I$ is an ESS if for all strategies $J$, $E_I(I) > E_I(J)$ and if $E_I(I) = E_I(J)$ then $E_J(I) > E_J(J)$.

An example of this evolution of strategies is the classic Hawk-Dove game [39] shown below in Box 1. If a hawk were to appear through mutation or migration in a

population made up completely of doves, the Hawk would would have a higher fitness and be able to reproduce readily. The pure dove strategy is therefore not an ESS. Similarly, in a population full of Hawks who are engaging in fitness-reducing combat, a dove would have higher fitness as they do not pay a cost to retreat from a Hawk. The pure hawk strategy is therefore not an ESS, and implies that the ESS would be a mixed strategy if it exists.

Essentially, Smith and Price extended the domain of game theory by removing the rationality or choice of strategy from the players of the game. This is a much more reasonable approach when applied to uncoordinated games as individuals often do not know the exact strategy of the remainder of the population. Instead, by allowing strategies to develop we can investigate the stability of strategy sets over time.

Evolutionary game theory has naturally been applied to evolutionary processes in nature, however it has been extended into economics as well as psychology and sociology. Recently there has been a peaked interest in how humans change behaviour when faced with disease [1, 2, 24, 27, 31]. For example, the recent outbreaks of measles in the UK have prompted epidemiologists to study why and when individuals cease to vaccinate [16]. This behaviour may be partly explained by individuals basing vaccination decisions on perceived risk of morbidity or mortality from infection. Initially when an infectious agent is common in a population, vaccination is widely used as a source of protection until incidence is reduced. At these lower levels, individuals perceive lower risks of infection and the monetary, personal or societal costs of vaccination may be relatively higher causing a drop in vaccination coverage. This drop in the population's protection against the disease will increase the likelihood of subsequent outbreaks through creating of a pool of susceptible individuals repeating the cycle. It is therefore natural to use evolutionary game theory instead of static game theory as a tool to explore vaccination behaviour as it allows for changes in behaviour based on the current state of the population's health. One way that evolutionary game theory has been used to study vaccination behaviour is through the use of replicator or imitation dynamics. These equations allow individuals to switch between available strategies by sampling other available strategies in the population. Should an individual meet someone with a different strategy and higher payoff, that

individual will switch to the other strategy with probability proportional to the gain in payoff. Using imitation dynamics, Bauch studied a model for pertussis and found that their model was able to reproduce features of pertussis vaccine uptake following a vaccine scare in England and Wales in the 1970s [1].

Without seasonal forcing, this model was able to produce persistent oscillations causing subsequent outbreaks. These similarities between the proposed model and current available data further support the need to include game theory when modeling human behaviour in regards to vaccination decisions (or other individual-based decisions). In particular, the author notes that countries with high vaccination voluntary vaccination coverage cannot be taken for granted. This statement is supported by many authors who suggest that voluntary vaccination programs are not sufficient to eradicate disease [3, 30, 44, 48]. Bauch and Bhattacharyya [2] demonstrate using imitation dynamics how it is possible that vaccine scares become more common as the eradication threshold for diseases is approached. By using social learning (imitation dynamics) and feedback of incidence on vaccinating behaviour the authors showed that their model was the most parsimonious fit to vaccine-scare data in comparison to a model without social learning or feedback. All of these studies suggest that voluntary vaccination of influenza would not be expected to aid in its eradication even if a universal vaccine were made available. In this chapter, we will explore the imitator equations in the context of influenza and demonstrate the complex dynamics that can arise. The chapter begins by defining the model equations and assumptions, followed by an analysis of equilibrium points when possible. The imitation parameters are then studied through numerical analysis and numerical simulations and sensitivity analysis are conducted. We will further analyze the model's sensitivity by estimating their Lyapunov exponents. The model in this chapter will then be used in Chapter 6, integrated with the decaying memory function discussed in Chapter 3.

**Box 1: Hawk–Dove game**

We will consider the Hawk–Dove game initially proposed by Smith and Price [39]. The hawks and doves do not represent two different species, but rather two different behaviours in one species of animal. The dove behaviour is to retreat whenever they encounter a hawk, paying zero cost of fitness while the expected payoff for a hawk in a hawk-dove matching is a gain of $G$. When a dove encounters another dove, both display until one retreats with equal probability. The winner takes away a gain in fitness of $G$, and therefore the expected payoff of two doves competing is $\frac{G}{2}$. When two hawks compete, they display and combat each other until one of them retreats (with equal probability). The hawks pay a cost $C$ from the injuries sustained in battle, and the winner gains $G$. The expected payoff for a hawk-hawk matching is therefore $\frac{G-C}{2}$ (where it is assumed $G - C < 0$). The payoff matrix for the above situation is given below.

| | $Hawk$ | $Dove$ |
|---|---|---|
| $Hawk$ | $\left(\frac{G-C}{2}, \frac{G-C}{2}\right)$ | $(G, 0)$ |
| $Dove$ | $(0, G)$ | $\left(\frac{G}{2}, \frac{G}{2}\right)$ |

(17)

Of particular interest, which strategy will individuals choose over an infinite number of matchings? In a population consisting entirely of hawks, individuals are decreasing their fitness with every matching. Therefore if a dove were introduced into the population, it would maintain a fitness of 0 by retreating with every hawk encounter (receiving a higher payoff). There is therefore incentive for hawks to switch behaviour. Similarly if a hawk were introduced into a population consisting only of doves, the hawk would receive a higher payoff than the doves showing an incentive to switch to the hawk strategy. The evolutionary stable strategy would therefore be given by a mixed strategy (consistent with the mixed Nash equilibrium).

## 5.1 Model with Imitation Dynamics

We will now consider a model in which individuals choose to vaccinate based on the infection prevalence, and the associated costs of infection and vaccination. We will study a model which modifies the risk of infection linearly and explore how the various parameters effect the outcome of an epidemic. We will consider a large population with frequency-dependent transmission, where individuals are equally susceptible and well-mixed. Individuals compare their vaccination strategy with rest of the population at a rate $\alpha$ and change strategies in proportion to the expected gain in payoff by switching strategies ($\kappa$ being the proportionality constant). To deviate slightly from the model proposed by Bauch, we will include the perceived costs of both vaccination and infection. We have chosen to scale the perceived costs as their value varies for each person, and this normalizes the cost of each outcome. We will assume that the cost of vaccination ($c_v$) is fixed, therefore the expected cost to vaccinate $E_V = -c_v$. Non-vaccinators pay a cost $c_i$, which is modified by a function $f(I)$ and the sensitivity to behavioural changes in response to infection prevalence $m$. The expected costs of the vaccinator and non-vaccinator strategies are

$$E_V = -c_v \qquad E_N = -c_i m f(I).$$

The expected gain in payoff from switching from a non-vaccinator to a vaccinator strategy ($\Delta E$) is therefore

$$\Delta E = E_V - E_N = -c_v + c_i m f(I).$$

To allow for more freedom in the scales of the costs of infection and vaccination, we will rescale by the total cost of each strategy ($c_v + c_i$) giving

$$\Delta E = E_V - E_N = -r_v + r_i m f(I) \tag{18}$$

where $r_v = \frac{c_v}{c_v + c_i}$ and $r_i = \frac{c_i}{c_v + c_i}$. Individuals sample other strategies at rate $\alpha$, and change strategies in proportion to the expected gain (or loss) in payoff. Therefore, the equations describing the change in vaccination behaviour is given by

$$x' = \alpha\kappa x(1-x)\Delta E$$

where $\kappa$ is a constant of proportionality. We denote $k = \alpha\kappa$ as the mixed imitation rate. Due to the highly connected nature of the models studied in this and later chapters, we have chosen to vaccinate under mass-action vaccination. It is important to note that $x$ represents the number of individuals actively seeking vaccination and not the direct proportion of vaccinators, since individuals will vary their strategy over time (we will refer to $x$ as the proportion of "vaccinators" in later figures). The differential equations resulting from the above description and a coupled $SIRVS$ model are provided below in system (19) with the following assumptions:

1. Individuals become infected after contact with an infected individual at rate $\beta$ under frequency-dependent transmission.

2. Infected individuals remain infectious for $\frac{1}{\gamma}$ days before recovering and moving to the recovered ($R$) class.

3. Recovered individuals maintain immunity to infection for $\frac{1}{\psi}$ days before immunity wanes and individuals return to the susceptible class.

4. Individuals sample and switch to strategies with higher payoff (according to the payoff functions defined in equation (18)) at mixed rate $k = \alpha\kappa$.

5. Susceptible individuals vaccinate at variable rate $x$ through mass-vaccination and move to the vaccinated class ($V$).

6. Vaccinated individuals maintain immunity to infection for $\frac{1}{\phi}$ days before immunity wanes and individuals return to the susceptible class.

$$\begin{aligned} S' &= \Lambda - \mu S - xS - \beta SI + \phi V + \psi R \\ I' &= \beta SI - \mu I - \gamma I \\ R' &= \gamma I - \mu R - \psi R \\ V' &= xS - \mu V - \phi V \\ x' &= kx(1-x)\left(-r_v + \frac{r_i m I}{N}\right) \end{aligned} \tag{19}$$

We have used direct incidence of influenza as a modifier of the risk of infection, however other functions have been used and analyzed [28]. The associated $SIRVS$ model (without imitation dynamics) does not have sustained oscillations for any positive parameter values. However, by including imitation dynamics we are able to destabilize all equilibrium points. We will next carry out stability analysis of the equilibrium points, explore the imitation parameters for a single season of influenza and run numerical simulations of potential strains of influenza.

## 5.2 Analysis

The system of equations outlined in (19) has two disease-free equilibrium points corresponding to the pure-vaccinator and non-vaccinator strategies. This system also gives rise to three endemic equilibrium points corresponding to disease persistence with pure vaccination, without vaccination and a mixed strategy in the population. Under certain parameter values, all five of these equilibrium points can be destabilized leading to periodic dynamics. We begin by demonstrating that the positive orthant is positively invariant under the flow of system (19), then show the necessary conditions for stability of both disease-free equilibrium points and provide conditions on the existence of the endemic equilibrium points and local asymptotic stability of the non-vaccinator endemic equilibrium.

**Proposition 5.2.1.** *The region* $\Gamma = \{(S, I, R, V, x) \in \mathbb{R}^4 \times [0,1] \mid S, I, R, V \geq 0\}$ *is positively invariant and bounded for system* (19).

*Proof.* This follows directly from the construction of the model. When any of the transition states are empty, there can be no removal from that state since all negative terms are proportional to the state itself. Similarly, the derivative of $x$ is null at the boundaries of the region and therefore cannot cross the boundary of the region. Furthermore, by summing the population state variables, we obtain $N' = \Lambda - \mu N$ and $N(t) = \frac{\Lambda}{\mu}(1 - e^{-\mu t}) + N_0 e^{-\mu t}$. We must therefore have that $S, I, R, V \leq \max\{N_0, \frac{\Lambda}{\mu}\}$ for all time, and thus the region $\Gamma$ is bounded. □

**Proposition 5.2.2.** *The disease-free equilibria for system* (19) *are given below*

$$\begin{aligned} X^* &= (S^*, I^*, R^*, V^*, x^*) = \left(\frac{\Lambda}{\mu}, 0, 0, 0, 0\right) \\ \bar{X} &= (\bar{S}, \bar{I}, \bar{R}, \bar{V}, \bar{x}) = \left(\frac{\Lambda(\mu+\phi)}{(\mu+1)(\mu+\phi)-\phi}, 0, 0, \frac{\Lambda}{(\mu+1)(\mu+\phi)-\phi}, 1\right). \end{aligned} \tag{20}$$

*If $\mathcal{R}_0 = \frac{\beta}{\mu+\gamma} < 1$, then $X^*$ is asymptotically stable for initial conditions $X \neq \bar{X}$; otherwise, it is unstable. The pure-vaccinator disease-free equilibrium $\bar{X}$ is always unstable.*

*Proof.* We will use the same proof method for the global stability of $X^*$ outlined in Chapter 2. One modification will need to be made, since the theorem requires a unique disease-free equilibrium. Instead, we will show again that the region $U = \{(S, I, R, V, x, ) \in \mathbb{R}_0^{5+} | I = 0\}$ is asymptotically stable. Using $L = \frac{1}{2}I^2$, we have that $L$ is positive semi-definite and the time derivative of $L$ is negative semi-definite in the sense of Theorem 2.1.4. Solutions also become trapped in the region $\{(S, I, R, V, x) \in \mathbb{R}_0^{4+} \times [0, 1] | S, I, R, V \leq \frac{\Lambda}{\mu}\}$. Solution must therefore approach $U$ asymptotically. Next we must show that solutions all converge asymptotically to the non-vaccinator disease-free equilibrium $X^*$. First, we will show that solutions cannot converge to the pure-vaccinator disease-free equilibrium. For a given value of $r_v \neq 0$, as the infection prevalence decreases to zero through $\frac{r_v N}{r_i m}$, the sign of $x'$ becomes negative. Below this threshold value, it is impossible for the proportion of vaccinators to increase, and we have $\lim_{t\to\infty} x = 0$.

Substituting $I = x = 0$ into system (19), we get that $R' < 0$ and $V' < 0$. It follows that $\lim_{t\to\infty} R = \lim_{t\to\infty} V = 0$ and that $\lim_{t\to\infty} S = \lim_{t\to\infty} \left(\frac{\Lambda}{\mu} - I - R - V\right) = \frac{\Lambda}{\mu}$.

Therefore, for initial conditions in $U\backslash\{\bar{X}\}$, solutions converge to the non-vaccinator disease-free equilibrium $X^*$. $X^*$ is therefore asymptotically stable for initial conditions $X \neq \bar{X}$.

We will provide a more formal proof that $\bar{X}$ is unstable. The Jacobian matrix of system (19) is

$$J = \begin{bmatrix} -\mu - x - \frac{\beta I}{N} & -\frac{\beta S}{N} & \psi & \phi & -S \\ \frac{\beta I}{N} & -\mu - \gamma + \frac{\beta S}{N} & 0 & 0 & 0 \\ 0 & \gamma & -\mu - \psi & 0 & 0 \\ x & 0 & 0 & -\mu - \phi & S \\ 0 & \frac{kx(1-x)r_i m}{N} & 0 & 0 & k(1-2x)\left[-r_v + \frac{r_i m I}{N}\right], \end{bmatrix}$$

$J(\bar{X} - \lambda I) =$

$$\begin{bmatrix} -\mu - 1 - \lambda & -\frac{\Lambda\beta(\mu+\phi)}{N((\mu+1)(\mu+\phi)-\phi)} & \psi & \phi & -\frac{\Lambda(\mu+\phi)}{(\mu+1)(\mu+\phi)-\phi} \\ 0 & -\mu - \gamma + \frac{\Lambda\beta(\mu+\phi)}{N((\mu+1)(\mu+\phi)-\phi)} - \lambda & 0 & 0 & 0 \\ 0 & \gamma & -\mu - \psi - \lambda & 0 & 0 \\ 1 & 0 & 0 & -\mu - \phi - \lambda & \frac{\Lambda(\mu+\phi)}{(\mu+1)(\mu+\phi)-\phi} \\ 0 & 0 & 0 & 0 & kr_v - \lambda. \end{bmatrix}$$

with characteristic equation given by

$$\begin{aligned}(kr_v - \lambda)(-\mu - \psi - \lambda)\left(\frac{\Lambda\beta(\mu+\phi)}{N((\mu+1)(\mu+\phi)-\phi)} - \mu - \gamma - \lambda\right) \\ \times \left((-\mu - 1 - \lambda)(-\mu - \phi - \lambda) - \phi\right) = 0.\end{aligned} \tag{21}$$

For $\bar{X}$, there is always at least one positive eigenvalue $\lambda_i = kr_v > 0$. Therefore the pure-vaccinator disease-free equilibrium is always unstable.

□

The instability of $\bar{X}$ make intuitive sense from the construction of the imitation dynamics. In a population with no incidence of infection, the non-vaccinator strategy will always have a larger payoff. Individuals will thus switch to the non-vaccinator strategy, which will become the evolutionary stable strategy.

**Proposition 5.2.3.** *The endemic equilibria are*

$$X_E = \left( \frac{\Lambda(\mu+\gamma)}{\mu\beta}, \frac{\Lambda r_v}{\mu r_i m}, \frac{\Lambda r_v \gamma}{\mu(\mu+\psi) r_i m}, \right.$$
$$\left. \frac{\Lambda(r_i m(\mu+\psi)(\beta-\mu-\gamma) - r_i m(\mu+\gamma)(\mu+\psi) - \beta r_v(\mu+\psi+\gamma))}{\mu\beta r_i m(\mu+\psi)}, \frac{(\mu+\phi)V_E}{S_E} \right)$$
$$X_E^* = \left( \frac{\Lambda(\mu+\gamma)}{\mu\beta}, \frac{\Lambda(\mu+\psi)(\beta-\mu-\gamma)}{\mu\beta(\mu+\psi+\gamma)}, \frac{\Lambda\gamma(\beta-\mu-\gamma)}{\mu\beta(\mu+\psi+\gamma)}, 0, 0 \right)$$
$$\bar{X}_E = \left( \frac{\Lambda(\mu+\gamma)}{\mu\beta}, \frac{\Lambda(\mu+\psi)((\beta-\mu-\gamma)(\mu+\phi)-(\mu+\gamma))}{\mu\beta(\mu+\phi)(\mu+\psi+\gamma)}, \frac{\gamma}{\mu+\psi} I_E, \frac{\Lambda(\mu+\gamma)}{\mu\beta(\mu+\phi)}, 1 \right).$$

*The equilibrium $X_E$ exists if and only if*

$$r_i \geq \frac{\beta(\mu+\psi+\gamma)}{m(\mu+\psi)(\beta-\mu-\gamma)+\beta(\mu+\psi+\gamma)} \equiv r^*.$$

*The equilibrium $X_E^*$ is locally asymptotically stable whenever $X_E$ doesn't exist and $\mathcal{R}_0 > 1$, otherwise it is unstable. The pure-vaccinator endemic equilibrium ($\bar{X}_E$) exists if and only if*

$$\frac{(\beta-\mu-\gamma)(\mu+\phi)}{\mu+\gamma} > 1.$$

*Proof.* For the endemic equilibrium to remain in $\Gamma$, it is required that all entries are positive. Therefore we must have

$$r_i m(\mu+\psi)(\beta-\mu-\gamma) - \beta r_v(\mu+\psi+\gamma) \geq 0.$$

Since we have chosen to scale the risks, we have that $r_i + r_v = 1$. Therefore we have

$$r_i m(\mu+\psi)(\beta-\mu-\gamma) + \beta r_i(\mu+\psi+\gamma) \geq \beta(\mu+\psi+\gamma)$$
$$r_i \geq \frac{\beta(\mu+\psi+\gamma)}{m(\mu+\psi)(\beta-\mu-\gamma)+\beta(\mu+\psi+\gamma)}.$$

The existence of $X_E$ is treated in the same way to obtain the condition outlined above. Next we will show local asymptotic stability of the endemic equilibrium $X_E^*$. The Jacobian of system (19) at $X_E^*$ is given by

$$J(X_E^* - \lambda I) =$$
$$\begin{bmatrix} -\mu - \frac{\beta I_E^*}{N} - \lambda & -\frac{\beta S_E^*}{N} & \psi & \phi & -S_E^* \\ \frac{\beta I_E^*}{N} & -\mu - \gamma + \frac{\beta S_E^*}{N} - \lambda & 0 & 0 & 0 \\ 0 & \gamma & -\mu - \psi - \lambda & 0 & 0 \\ 0 & 0 & 0 & -\mu - \phi - \lambda & S_E^* \\ 0 & 0 & 0 & 0 & k\left[-r_v + \frac{r_i m I_E^*}{N}\right] - \lambda \end{bmatrix}.$$

The associated characteristic equation is

$$(-\mu - \phi - \lambda)\left(k\left[-r_v + \frac{r_i m I_E^*}{N}\right] - \lambda\right)\left(\lambda^2 + \left(2\mu + \psi + \gamma + \frac{\beta I_E^*}{N} - \frac{\beta S_E^*}{N}\right)\right)\lambda$$
$$+ (\mu + \psi)\left(\mu + \gamma + \frac{\beta I_E^*}{N} - \frac{\beta S_E^*}{N}\right) + \frac{\beta \gamma I_E^*}{N}\Bigg) = 0.$$

First we will examine the eigenvalue associated to the imitation dynamics. For this eigenvalue to have negative real part, it is required that

$$\begin{aligned} -r_v + \frac{r_i m I_E^*}{N} &< 0 \\ \frac{r_i m(\mu + \psi)(\beta - \mu - \gamma)}{\beta(\mu + \psi + \gamma)} &< r_v \\ r_i \frac{m(\mu + \psi)(\beta - \mu - \gamma) + \beta(\mu + \psi + \gamma)}{\beta(\mu + \psi + \gamma)} &< 1 \\ r_i &< \frac{\beta(\mu + \psi + \gamma)}{m(\mu + \psi)(\beta - \mu - \gamma) + \beta(\mu + \psi + \gamma)}. \end{aligned}$$

Therefore, the endemic equilibrium $X_E^*$ is unstable whenever $X_E$ exists. We will next examine the quadratic equation. The roots have negative real part if and only if all coeffecients are strictly positive. This gives two conditions for these eigenvalues. First, we must have

$$\begin{aligned} 0 &< 2\mu + \psi + \gamma + \frac{\beta I_E^*}{N} - \frac{\beta S_E^*}{N} \\ 0 &< 2\mu + \psi + \gamma + \frac{(\mu + \psi)(\beta - \mu - \gamma) - (\mu + \gamma)(\mu + \psi + \gamma)}{\mu + \psi + \gamma} \end{aligned}$$

which simplifies to the following condition:

$$\epsilon_1 = \mathcal{R}_0 + \frac{\mu(\mu+\psi+\gamma)}{(\mu+\psi)(\mu+\gamma)} > 1.$$

Next we must also have

$$(\mu+\psi)\left(\mu+\gamma+\frac{\beta I_E^*}{N}-\frac{\beta S_E^*}{N}\right)+\frac{\beta\gamma I_E^*}{N} > 0.$$

This expression simplifies to the following condition:

$$\epsilon_2 = \frac{\beta}{\mu+\gamma} > 1.$$

Therefore the associated eigenvalues have negative real part if and only if

$$\min\{\epsilon_1, \epsilon_2\} = \epsilon_2 = \mathcal{R}_0 > 1.$$

Hence, if $X_E$ doesn't exist and $\mathcal{R}_0 > 1$ then $X_E^*$ is locally asymptotically stable.

□

Having used evolutionary game theory to model the spread of influenza, we must ask what constitutes an evolutionary stable strategy. When the system reaches an endemic equilibrium, would the ESS simply be the proportion of vaccinated individuals? The definition of an ESS for deterministic and stochastic models has been debated, and modifications must be made for the definitions to make sense; do individuals play a mixed strategy to vaccinate with a certain probability $p$ or is a proportion $p$ of the population playing a pure-vaccinator strategy? In a deterministic model at equilibrium, the number of individuals vaccinated or playing a pure-vaccinator strategy will frequently be a non-integer value, which is problematic for the definitions of the ESS. If the number of individuals vaccinated were to be rounded off, it is possible that this would shift the equilibrium enough to allow for individuals to marginally increase their payoff by switching strategies. The ESS is therefore not attained by the population, as the distribution of strategies would oscillate back and forth around the non-integer value. This is the inherent problem when using deterministic models for evolutionary game theory, as it does not respect the definitions originally laid out

by Smith [39]. First, the definitions for evolutionary games were made for infinitely large populations. However, through the law of large numbers it has been suggested that results of evolutionary games with finite (but sufficiently large) populations have similar characteristics to their infinitely large counterparts [40]. Although stochastic models are an intuitively better fit for determining the ESS, utilizing imitation dynamics in deterministic models has shown to provide interesting dynamics. Special care should be taken when classifying an ESS when using deterministic models, and the sensitivity of the behaviour of systems to different population sizes should be studied. Different population sizes were simulated to ensure results are consistent but have been excluded from the analysis as they were qualitatively similar at larger population sizes. The next section will explore the imitation parameters for a single and multiple seasons of influenza and study sensitivity to initial conditions using Lyapunov exponents.

## 5.3 Numerical Simulations and Analysis

### 5.3.1 Simulations without waning immunity: exploration of imitation parameters

For this section, we will only consider a single season of influenza by setting $\phi = \psi = 0$. As with the simulations in previous chapters, graphs were created with Matlab using the Runge–Kutta(4,5) method. We will be choosing imitation parameters consistent with those chosen in Bauch [1]. The difficulty in determining an accurate value for the mixed imitation parameter $k$ is similar to the problem posed when building who-infects-whom contact matrices in the sense that the rate at which individuals sample other strategies is difficult to measure. The mixed imitation rate $k$ is able to alter the global dynamics of the system, since it is able to stabilize $x$ for sufficiently small values by slowing the change in vaccination behaviour and hence reduce oscillations. The sensitivity to prevalence of infection parameter $m$ also has the ability to alter global dynamics. The sensitivity parameter $m$ can be decreased to values at which any infection prevalence we will have $x' < 0$ and the proportion of those actively seeking

Table 5: Parameter values used for numerical simulations of system (8). Parameter values in this table are used for all simulations in this section unless otherwise stated.

| Parameter | Description | Simulation value | Ref. |
|---|---|---|---|
| $\mu$ | Human death rate | $\frac{1}{80 \cdot 365}$ | [46] |
| $\Lambda$ | Human birth rate | $10000\mu$ | Calculated |
| $\beta$ | Contact rate | 0.3 | [a] |
| $\gamma$ | Recovery rate | $\frac{1}{4}$ | [7] |
| $\psi$ | Rate of waning immunity (natural) | $\frac{1}{150}$ | [8][b] |
| $\phi$ | Rate of waning immunity (vaccine) | $\frac{1}{150}$ | [8][b] |
| $m$ | Sensitivity to prevalence | 0.8 | Assumed |
| $r_i$ | Risk of infection | $\geq 0.9$ | Assumed[c] |
| $k$ | Mixed imitation rate | Varied | Assumed |

[a] Contact rate was chosen to give values of $\mathcal{R}_0 \in (1, 2.5)$.
[b] Rates of waning immunity (vaccine and naturally induced) were chosen to be equal and last for five months corresponding to a month before and after peak activity.
[c]Risk of vaccination is excluded, as $r_v = 1 - r_i$.

vaccination decreases to zero. This reduces system (19) to an $SIRS$ model that has a globally stable disease-free or endemic equilibrium (dependent on $\mathcal{R}_0$). Similarly, the risk of vaccination $r_v$ (and consequently $r_i$) has the ability to restrict periodic dynamics. As seen in Chapter 4, if a vaccine carries a higher risk than infection (at any prevalence), no individual will choose to vaccinate corresponding to $x = 0$ and thus solutions approach a globally stable equilibrium point. We begin with exhibiting the effects of the imitation parameters of system (19) for a single season of influenza.

Figure 12 shows how increasing the imitation rate increases the total number of individuals infected over the course of a season. When the risk of infection is high

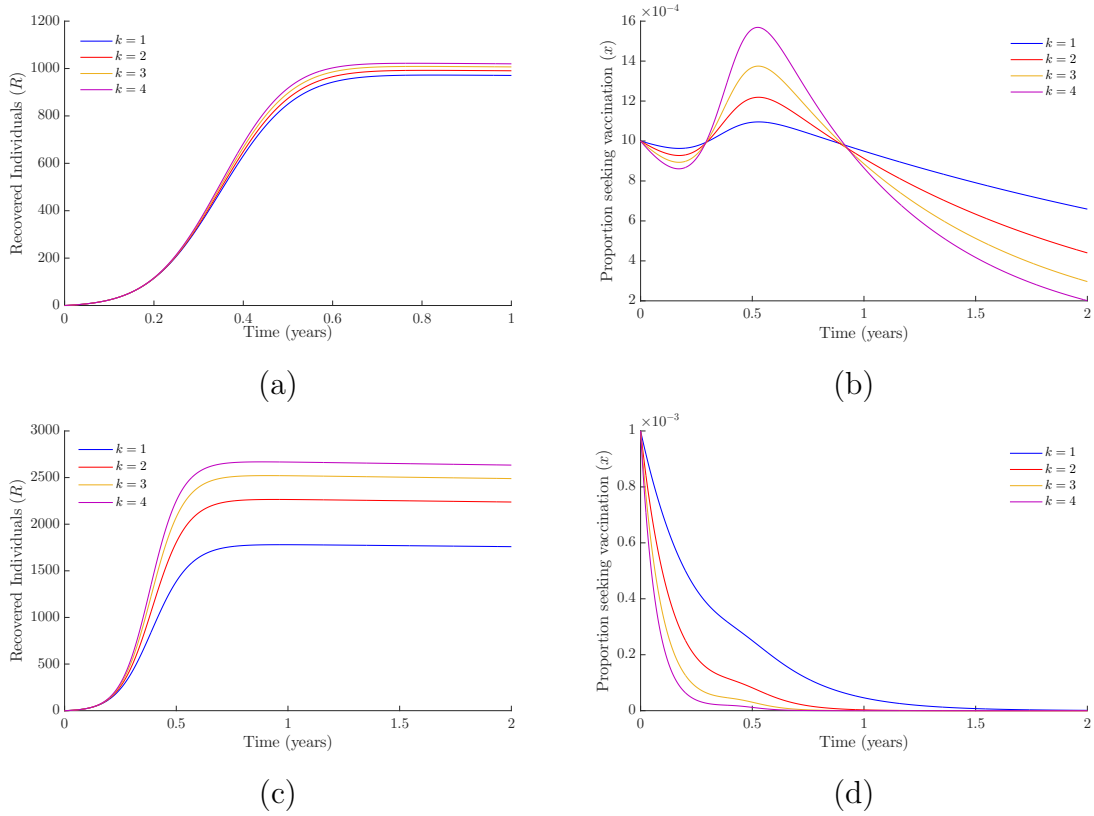


Figure 12: Time series of (a) recovered individuals and (b) the proportion of individuals seeking vaccination with low infection risk $r_i = 0.99$ as well as for (c) recovered individuals and (d) the proportion of individuals seeking vaccination with high infection risk $r_i = 0.999$ for various values of the mixed imitation rate ($k$). Simulations exclude the effects of waning immunity ($\psi = \phi = 0$). All other parameter values used are provided in Table 5.

(Figures 12a and 12b), initially there is no disease prevalence and individuals imitate the non-vaccinator strategy, as it has a higher payoff and thus $x$ decreases for faster imitation rates. This causes a slight drop in vaccination coverage as $k$ increases. Although the proportion of individuals seeking vaccination is higher during the epidemic for larger values of $k$, at this point it is too late to be protected by vaccination. The lower imitation rate slows the rate of change of $x$ which preemptively vaccinates more of the population. For lower risks of infection (Figures 12c and 12d), the incentive to vaccinate is not sufficient for individuals to switch strategies (corresponding to $x' < 0$). In this case, the proportion of individuals seeking vaccination decreases faster for higher values of $k$. This results in decreased vaccination coverage as the value of $k$ increases, producing an increased number of individuals infected over the season. As the risk of infection is increased further, a higher imitation rate will lead to higher vaccination coverage. This is due to a shift in the first intersection of the solution curves in Figure 12(b), individuals vaccinate earlier, providing more protection during the peak of the epidemic. This shows that when vaccines have a high enough perceived risk, individuals acting on imitation dynamics may delay vaccination until the epidemic occurs. It is therefore important to ensure that individuals perceive the vaccine to be safe in order to ensure coverage is achieved well before the threat of the epidemic occurs. Since the cost of infection is substantially higher than the cost of vaccination for influenza [13, 31], increases in the imitation rate for influenza vaccination behaviour in our model may lead to lower levels of coverage. Similarly to the risk of infection, an increase in the contact rate or the recovery period (and consequently the reproductive ratio) would result in increased protection for higher imitation rates. This is due to the resulting increase in the number of infected individuals, which modulates the risk of infection. We will next consider the effects of the sensitivity to the infection prevalence parameter, $m$.

In Figure 13, we find that $m$ has a small effect on the number of previously infected (recovered) individuals. This effect is decreased further as the mixed imitation rate ($k$) or the risk of infection increases. This was expected since as $m$ is increased, the threshold for changing vaccination behaviour is reached faster, leading to increased

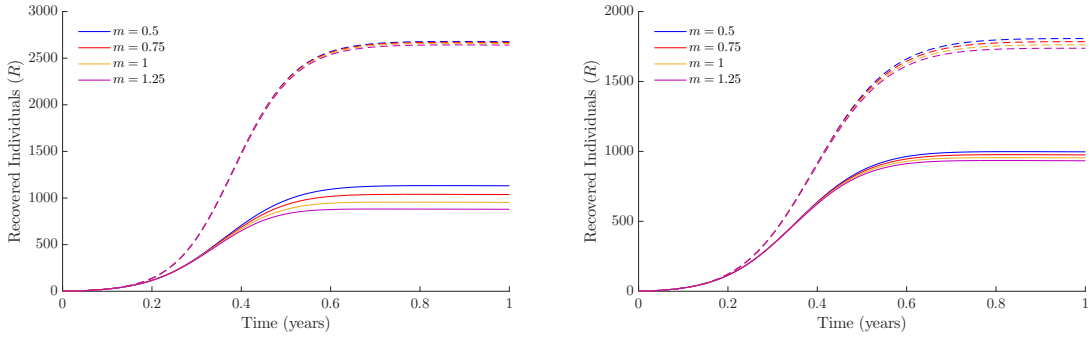


Figure 13: Time series of recovered individuals for a single season of influenza ($\phi = \psi = 0$) versus time for a range of the sensitivity to prevalence parameter ($m$) with (a) risk of infection $r_i = 0.99$ and (b) $r_i = 0.999$. Solid and dashed lines correspond to simulations with mixed imitation parameter $k = 1$ and $k = 4$, respectively. All other parameter values used are provided in Table 5.

vaccination coverage during the epidemic. As the risk of infection is increased, individuals vaccinate earlier in the epidemic and require fewer infected individuals present to trigger the switch. Larger differences in the values of $m$ would be required for higher values of the risk of infection to reproduce the differences observed in Figure 13. It is important to note that, although the sensitivity to infection prevalence does not change the number of infections significantly for the ranges studied, if decreased sufficiently low, it can ensure that the terms for infection risk are always inferior to the vaccination risk, leading to an increased number of infections.

### 5.3.2 Simulations with waning immunity

We ran numerical simulations with non-zero rates of waning immunity. Numerical simulations and graphs were created with Matlab using the Runge–Kutta(4,5) method with relative and absolute integration error tolerances set to $10^{-12}$ to ensure that solutions remain positive. This specification is important for these simulations, since $x$ is often close enough to zero to allow the approximations of $x$ to change sign. We will illustrate the stability results determined in Section 5.2 and show that, under certain

conditions, periodic dynamics occur without inclusion of seasonal forcing. As the risk of infection is decreased below $r^*$, such as in Figure 14a, solutions approach the pure non-vaccinator endemic equilibrium $X_E^*$ consistent with the analysis of Section 5.2 and with individuals not choosing to vaccinate when the risk of vaccination is sufficiently high. In Figure 14b, the risk of infection was chosen slightly above the value of $r^*$. In this case, solutions converge to the mixed-strategy endemic equilibrium $X_E$. The instability of $X_E^*$ is shown in Figure 15 for $r_i > r^*$ by running a simulation with initial conditions at $X_E^*$. In this case, solutions diverge from the non-vaccinator equilibrium ($X_E^*$), oscillate and converge to the mixed-strategy endemic equilibrium ($X_E$). Finally, as the risk of infection is increased further past $r_i$, such as in Figure 16, the mixed-strategy endemic equilibrium $X_E$ is destabilized; solutions diverge and approach a periodic orbit. Initially, when running simulations, we found erratic behaviour of solutions curves, leading us to believe there may be sensitive dependence on initial conditions. This possibility was supported through the literature, which suggested that chaos can arise from similar epidemic models which use a delayer kernel to report disease incidence [11]. We will demonstrate that the proposed model does not exhibit sensitivity to initial conditions as was initially suspected, due to solutions becoming temporarily negative.

### 5.3.3 Numerical Analysis using Lyapunov Exponents

Following a method described by Wolf et al. [47], we will numerically calculate the Lyapunov exponents of system (19). Lyapunov exponents are related to the convergence or divergence of nearby solutions. Wolf defines a system to be chaotic if a system has one or more positive Lyapunov exponents; however, to be conservative in using the term chaotic, we will identify systems with a positive Lyapunov exponent to be sensitive to initial conditions. Initial simulations showed that solutions could be sensitive to initial conditions, since solutions with nearby initial conditions eventually led to out-of-phase periodic dynamics. We will go on to show that our system is not sensitive to initial conditions, although initial numerical simulations suggested the possibility.

**Definition 5.3.1.** A dynamical system is said to be chaotic if it is sensitive to initial conditions, topologically transitivity (any open set will eventually overlap any other open set) and contains dense periodic orbits.

Chaos has been claimed for many dynamical systems by classifying any dynamical system with sensitivity to initial conditions as chaotic. The last two properties are extremely difficult to demonstrate for simple dynamical systems; consequently, we will only state that models with positive Lyapunov exponents determined from our numerical calculations are sensitive to initial conditions.

The above method works by tracking the long-term evolution of an infinitesimal $n$-sphere of initial conditions, which is deformed over time into an $n$-ellipsoid. Wolf defines the $i$th one-dimensional Lyapunov exponent in terms of the length of the ellipsoidal principal axis $p_i(t)$:

$$\lambda_i = \lim_{t\to\infty} \frac{1}{t} \log_2 \frac{p_i(t)}{p_i(0)}.$$

By tracking the length of each of the $n$ principal axes over time, we are precisely measuring the divergence of the $n$ solutions from the central initial condition. The difficulty in managing these $n$ vectors is that their direction is not well defined for a given exponent as the orientation of the $n$-ellipsoid changes continuously. In order to determine the Lyapunov exponents, the authors use a phase-space-plus-tangent-space approach; allowing the centre of the initial $n$-sphere to evolve according to the non-linear phase space while allowing the points on the surface of the $n$-sphere to evolve according to the linearized phase space. Wolf states that, in a chaotic system (which we will assume to mean a system sensitive to initial conditions as they had been defined previously), each of the $n$ vectors tend to fall along the direction of most rapid growth. This is problematic, because the initial orthonormal vectors tend to converge on the same direction, making them indistinguishable over time. In order to circumvent this problem, the authors repeatedly employ the Gram–Schmidt reorthonormalization (GSR) procedure on the $n$-dimensional vector frame (approximately once every orbit). This procedure does not affect the first vector; therefore it is continually seeking the direction of most rapid growth in the tangent space. The remaining vectors have their direction changed through the GSR procedure, and

therefore cannot seek out the direction of most rapid growth. However, the subspace spanned by the first $k$ vectors is unchanged by the GSR procedure and the $k$-volume defined by these vectors is proportional to $2^{\lambda_1 t+\lambda_2 t+\cdots+\lambda_k t}$. Beginning with determining the magnitude of the first vector, we can determine an estimate for the largest Lyapunov exponent (largest since it is following the path of most rapid growth); the remaining $k-1$ Lyapunov exponents can also be estimated using the values of the vectors before being orthonormalized. The author states that positive and zero Lyapunov exponents converge at roughly the same speed, while negative exponents converge much quicker. He goes on to suggest that, in practice, an asymptotic value of the Lyapunov exponent is attained when the mandatory zero exponent(s) (all smooth dynamical systems must have a zero exponent) are a few orders of magnitude smaller than the smallest positive exponent.

The reorthonormalization process was chosen to occur every $T = 10$ days, substantially more frequent than once per orbit, as suggested by Wolf [47]. In Figures 17a and 17b, we show the results of the analysis for parameter values that give periodic dynamics. This first analysis was run for $t = 2000$ years which did not provide clear asymptotic values of the largest Lyapunov exponent. However, since the other four exponents appear to converge to a negative value, this leaves the positive approximation to be the mandatory zero Lyapunov exponent (necessary due to the apparent stability of the limit cycle). This suggests that system (19) does not exhibit sensitivity to initial conditions, although early simulations of the model suggested the possibility. In Figure 17c, we show the same analysis for a lowered infection risk, which corresponds to a lack of periodic dynamics as a control. Lyapunov exponents converged rapidly to their negative (and zero) asymptotic values, consistent with what is expected of a system that converges to a fixed point.

### 5.3.4 Sensitivity Analysis

We will again use Latin hypercube sampling and partial rank correlation coefficients to determine the sensitivity of the model to its parameters with a sample size of $N = 1000$. For model (19), the expression for $\mathcal{R}_0$ is again too simple to provide

Table 6: Minimum and maximum values for PRCCs/LHS using uniform distribution.

| Parameter | Minimum | Maximum | Parameter | Minimum | Maximum |
|---|---|---|---|---|---|
| $\mu$ | $\frac{1}{90 \cdot 365}$ | $\frac{1}{70 \cdot 365}$ | $\psi$ | $\frac{1}{200}$ | $\frac{1}{100}$ |
| $\beta$ | 0.25 | 0.6 | $r_i$ | 0.9 | 0.999 |
| $\gamma$ | $\frac{1}{8}$ | $\frac{1}{4}$ | $m$ | 0.5 | 1.5 |

insight into the sensitivity of parameters. Therefore, we have chosen the output to be the number of infected individuals at the mixed-strategy endemic equilibrium ($I_E$). The results are shown in the Figures 18 and 19.

Parameter ranges were selected using the same method as in Chapter 3, with exception of two extra parameters. For the sensitivity to infection prevalence, values were chosen between 0.5 and 1.5, which are consistent with ranges studied by Bauch [1]. The risk of infection is difficult to quantify, as it varies significantly from person to person depending on age, risk group, past experience, personal beliefs and religious views. We have chosen a lower bound of 0.9 for the risk of infection ($r_v = 0.1$) and 0.999 as an upper bound ($r_v = 0.001$). Studies place the relative cost of vaccination as substantially lower than the relative cost of infection [13, 38]. The ranges chosen for $r_i$ are therefore much larger than required; however, due to the uncertainty of this parameter, we chose to maintain this range. The ranges are summarized in Table 6.

Since the number of infected individuals at the mixed-strategy endemic equilibrium is independent of many of the parameters, we have chose to use the stability condition $\frac{r^*}{r_i}$ as the output for sensitivity analysis. The only two sensitive parameters were found to be the risk of infection and the recovery rate. These results were expected, as the risk of infection is a key factor in determining the vaccination behaviour of the population. When the infection risk is low (higher vaccination risk), Figure 19a shows that the majority of points lead to a locally asymptotically stable non-vaccinator endemic equilibrium. For higher infection risks, the mixed-strategy endemic equilibrium becomes locally asymptotically stable. Although the stability

parameter is sensitive to the risk of infection, it was given a larger range than necessary. We also note that, as the recovery rate is increased, the non-vaccinator endemic equilibrium gains local asymptotic stability (results shown in Figure 19b). This is consistent with what is expected as the number of infections and consequently the risk of infection would be decreased, leading to a decrease in vaccination coverage. Sensitivity analyses were also run on the number of vaccinated individuals at the mixed-strategy endemic equilibrium ($X_E$) and showed that the risk of infection was not a sensitive parameter.

## 5.4 Discussion

These numerical simulations and analyses show that periodic dynamics can arise when introducing equations that model human behaviour and personal risk-assessment. These periodic dynamics are a direct consequence of the free-rider dilemma, since individuals may increase their payoff by ceasing vaccination behaviours. This drop in vaccination coverage is sufficient to create subsequent outbreaks.

The issue that arises with the imitation-dynamics equations is that the behaviour is sensitive to changes in prevalence; as soon as the number of infective individuals decreases past a certain threshold value, the number of individuals who choose the vaccinator strategy decreases rapidly to zero. Although this can be slowed through varying parameters, in reality the number of individuals who are vaccinators does not decrease to zero in between epidemics. This occurs because the humans in this model are reactive to increases in prevalence in the current season, whereas individuals in society base their vaccination decisions on a variety of factors. This motivates the need to introduce a secondary mechanism to control the speed at which individuals change vaccination strategies. In the following chapter, we will reintroduce the memory function used in Chapter 3 into the imitation dynamic model.

As previously discussed, the notion of an evolutionary stable strategy is not necessarily suitable for deterministic models such as the ones we explore in this study. This is partly due to the need for infinitely large populations when employing evolutionary game theory. It has been shown through the law of large numbers that conclusions

drawn from these models still hold for large populations. Other factors such as periodicity of solutions also cause difficulty in determining an ESS. For example, when periodic dynamics arise, there is no fixed strategy that maintains a highest payoff for all time. It may therefore be necessary to extend the definition of evolutionary stable strategies for vaccination models with periodic solutions by redefining the ESS as the time at which an individual chooses to vaccinate every year.

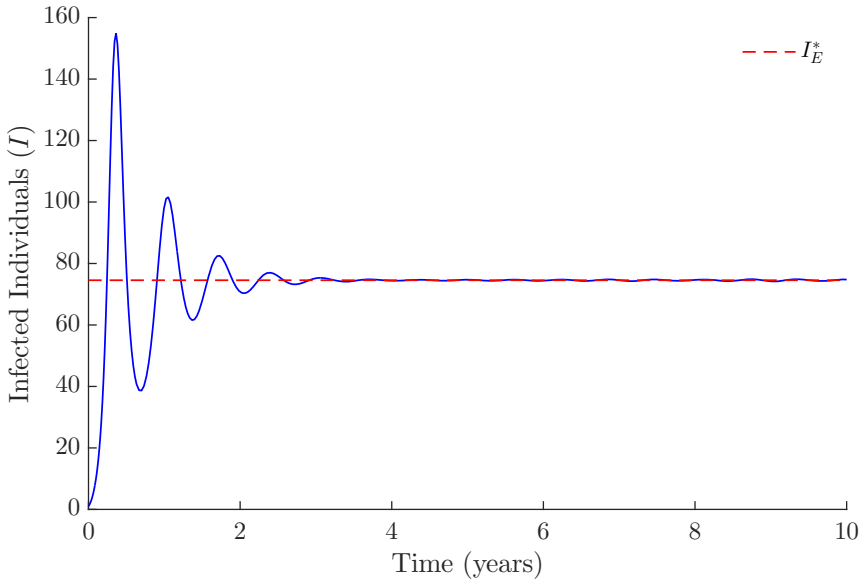


(a)

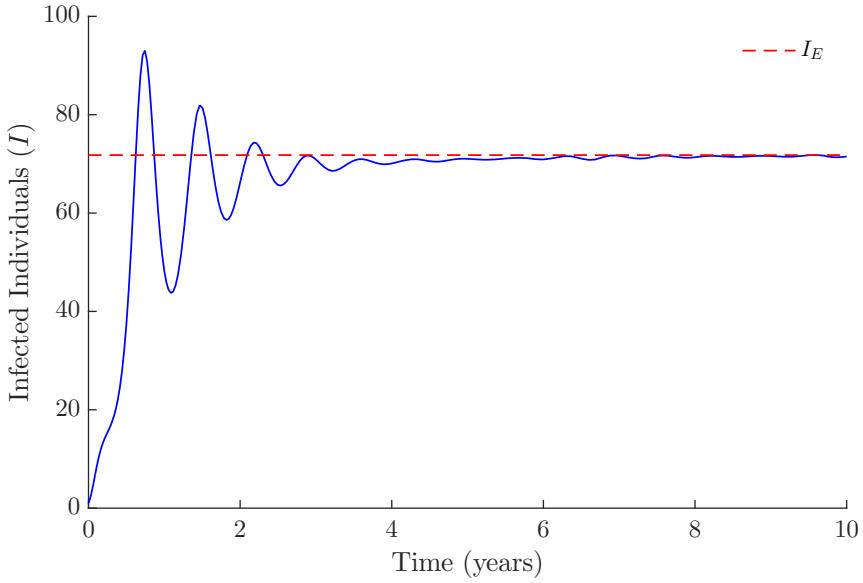


(b)

Figure 14: Time series of infected individuals with (a) $r_i = 0.99 < r^*$, where solutions oscillate and converge to the non-vaccinator endemic equilibrium ($X_E^*$), and (b) with $r_i = 0.995 > r^*$, where solutions oscillate around and converge to the mixed-strategy endemic equilibrium ($X_E$). All unspecified parameter values used are provided in Table 5.

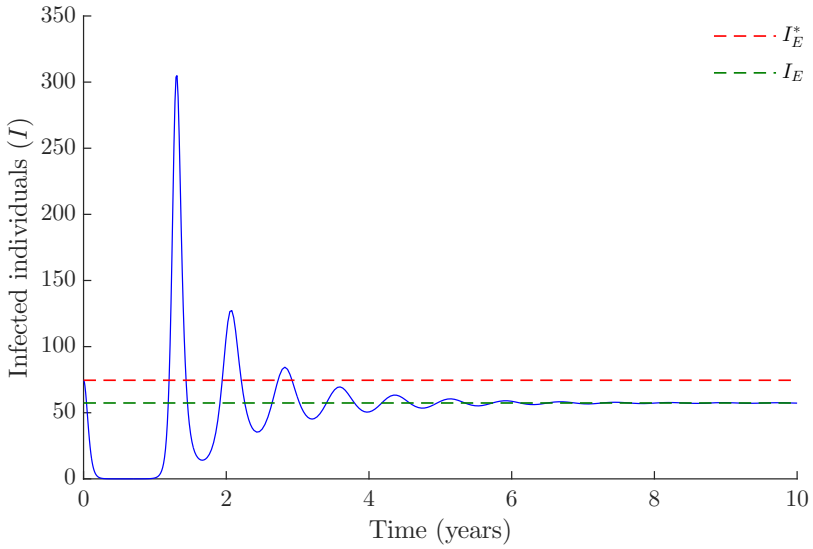


Figure 15: Time series of infected individuals with $r_i = 0.995 > r^*$. Initial conditions were set at the non-vaccinator endemic equilibrium ($X_E^*$). Solutions diverge from this equilibrium and converge towards the mixed-strategy endemic equilibrium ($X_E$). All unspecified parameter values used are provided in Table 5.

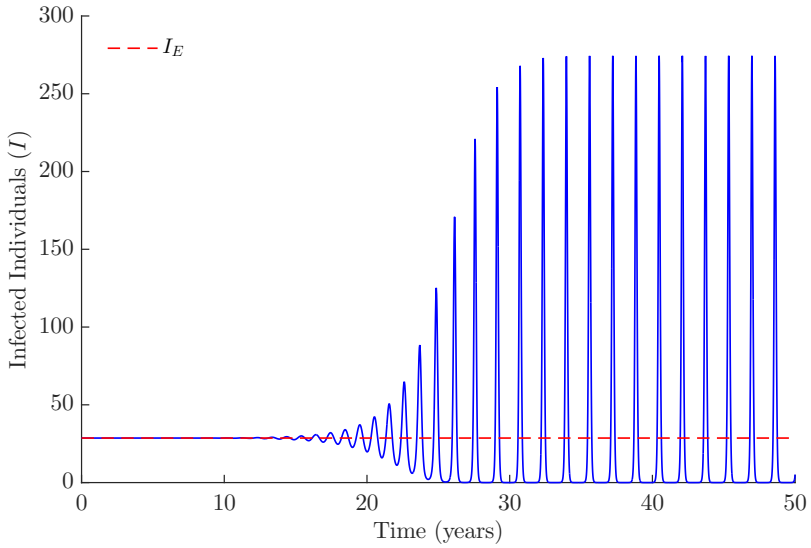


Figure 16: Time series of infected individuals with $r_i = 0.998 > r_i^*$ with initial conditions at the mixed-strategy endemic equilibrium $X_E$. Solutions diverge and reach a periodic orbit. All unspecified parameter values used are provided in Table 5.

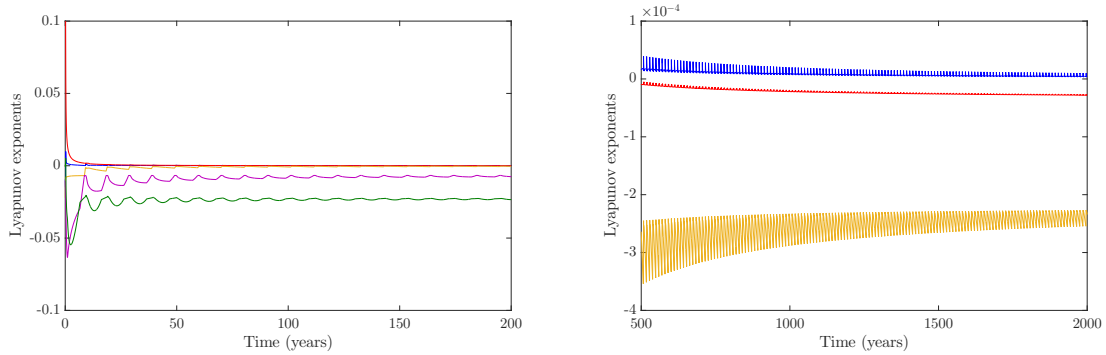


(a)




(b)

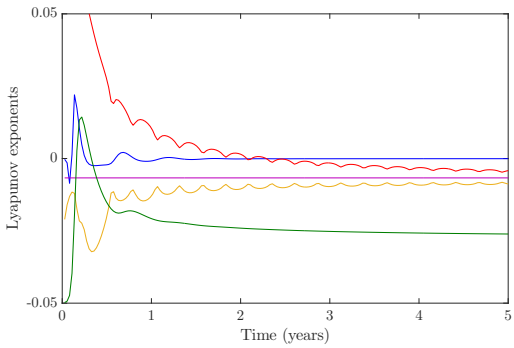


(c)

Figure 17: Results of numerical estimation of Lyapunov exponents of system (19) with reorthonormalization occurring every 10 days. Risk of infection of $r_i = 0.999$ is used for (a) and (b) while $r_i = 0.95$ in (c). Parameter values used for these analyses are given in Table 5.

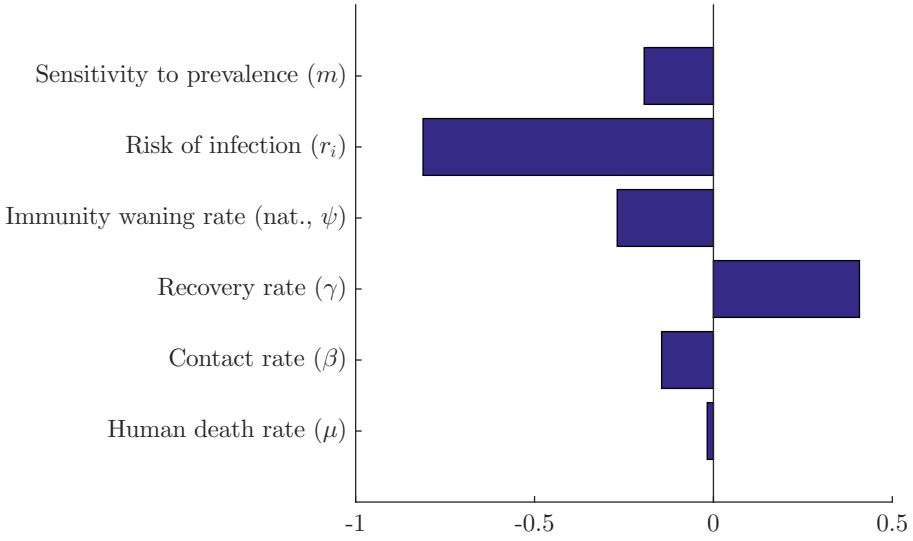


Figure 18: PRCC sensitivity analysis with $N = 1000$ simulations for listed parameters of system (19) using ranges from Table 6 and the stability parameter of $X_E^*$: $\frac{r^*}{r_i}$.

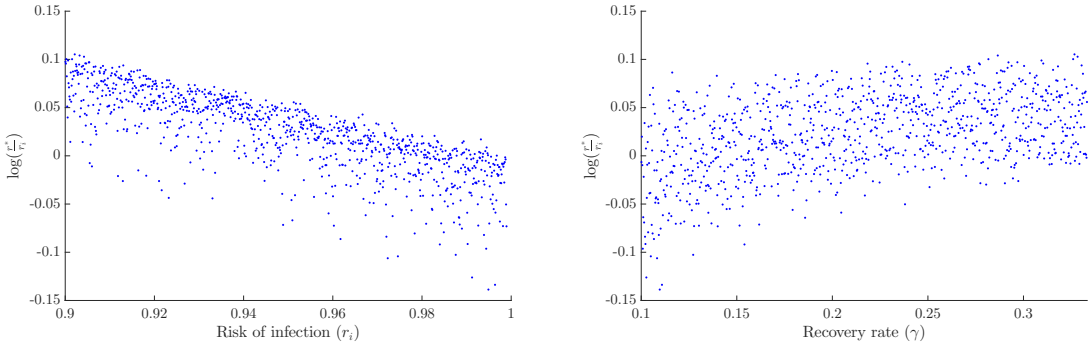


(a) (b)

Figure 19: Dependence of $\frac{r^*}{r_i}$ on the two most sensitive parameters (determined from the PRCCs) of system (19): (a) the risk of infection ($r_i$) and (b) the recovery rate ($\gamma$). Results were generated over $N = 1000$ simulations with parameter ranges shown in Table 6.

# Chapter 6

# Imitation dynamics with memory

In this chapter, we will integrate the memory function explored in Chapter 3 with the imitation dynamics of Chapter 5. The model presented in Chapter 5 only allowed individuals to respond to a current threat, while individuals also often base vaccination decisions on past experience with the virus. By allowing individuals in our models to remember the average number of cases over a certain number of years, we expect that the vaccination behaviours will be less erratic and more proactive. The model we will present is connected in such a way that stability analysis is not possible; however, we will show that, under similar conditions to the models presented in Chapters 3 and 5, periodic dynamics occur without seasonal forcing. The results of this chapter support the claim that the free-rider dilemma leads to failure of voluntary vaccination campaigns in the long term when individuals act with self-interest. The following chapter is organized as follows. We will introduce the epidemic model equations and associated assumptions, followed by analysis of equilibria, numerical simulations and sensitivity analyses.

## 6.1 Model assumptions and equations

The previous game-theoretic model demonstrated how complex dynamics occur through introducing imitation dynamics. However, individuals rapidly switch to the non-vaccinator strategy in between influenza seasons. Individuals often make decisions

to vaccinate based on their perceived risk of infection over multiple seasons. By integrating the models from Chapters 3 and 5, we will allow individuals to base their vaccination decisions using their experience with infection over a fixed time period, allowing for a more controlled imitation dynamic equation. The model assumptions and equations are provided below:

1. Individuals die at rate $\mu$ and are born at rate $\Lambda = N \cdot \mu$ to ensure asymptotically constant population size.

2. Susceptible individuals ($S$) are infected upon contact with an infected individual at rate $\beta$ under the assumption of frequency-dependent transmission and are moved to the infected compartment ($I$).

3. Infectious individuals ($I$) remain infectious for $\frac{1}{\gamma}$ days before moving to the recovered compartment ($R$).

4. Recovered individuals ($R$) maintain infection-induced immunity for $\frac{1}{\psi}$ days before immunity wanes and individuals are moved back to the susceptible compartment ($S$).

5. The average number of infections over $\theta$ seasons ($M$) is used by the population to evaluate their risk.

6. Individuals sample other vaccination strategies at mixed imitation rate $k$, and switch behaviours proportionally to the expected payoff gain (so long as it is higher).

7. Susceptible individuals actively seeking vaccination ($x$) are vaccinated through mass-action vaccination at rate $\rho$ and are moved to the vaccinated compartment ($V$).

8. Individuals maintain vaccine-induced immunity for $\frac{1}{\phi}$ days before immunity wanes and individuals are moved back to the susceptible compartment ($S$).

$$
\begin{aligned}
S' &= \Lambda - \mu S - \frac{\beta SI}{N} - \rho x S + \psi R + \phi V \\
I' &= \frac{\beta SI}{N} - \mu I - \gamma I \\
R' &= \gamma I - \mu R - \psi R \\
V' &= \rho x S - \mu V - \phi V \\
M' &= \frac{\beta SI}{\theta N} - \eta M \\
x' &= kx(1-x)\left(-r_v + \frac{m r_i M}{N\theta}\right).
\end{aligned}
\tag{22}
$$

## 6.2 Analysis

The differential equations of system (22) are dependent on each other in such a way that we are not able to determine explicit values for the local stability of the endemic equilibria. However, we are able to obtain global stability of the disease-free equilibrium as we have done in previous chapters, and we also include conditions on the existence of endemic equilibria.

**Proposition 6.2.1.** *The region* $\Gamma = \{(S, I, R, V, M, x) \in \mathbb{R}^5 \times [0,1] | S, I, R, V, M \geq 0\}$ *is positively invariant and bounded.*

**Proposition 6.2.2.** *The disease-free equilibria of system* (22) *are given by*

$$
\begin{aligned}
X_0 &= \left(\frac{\Lambda}{\mu}, 0, 0, 0, 0, 0\right) \\
X^* &= \left(\frac{\Lambda(\mu+\phi)}{\mu(\mu+\phi+\rho)}, 0, 0, \frac{\Lambda\rho}{\mu(\mu+\phi+\rho)}, 0, 1\right).
\end{aligned}
$$

$X_0$ *is globally asymptotically stable whenever* $\mathcal{R}_0 = \frac{\beta}{\mu+\gamma} < 1$. *Otherwise, it is unstable. The pure-vaccinator disease-free equilibrium* $X^*$ *is always unstable.*

*Proof.* As discussed in previous chapters, global stability of the disease-free equilibrium is obtained as a consequence of Theorem 2.1.4. Proposition 6.2.1 shows that solutions eventually enter a bounded space. Using $L = \frac{1}{2}I^2$, we have that $L$ is positive semi-definite with negative semi-definite time derivative in the sense of Theorem

2.1.4. This ensures asymptotic stability of the hyperplane defined by $I = 0$. Along this hyperplane, we have $R', M' < 0$ and thus $\lim_{t\to\infty} R = \lim_{t\to\infty} M = 0$. The second disease-free equilibrium $X^*$ is always unstable through the natural lack of incentive to vaccinate without disease prevalence. Following the proof in Proposition 5.2.2, we have $\lim_{t\to\infty} x = 0$ and consequently $\lim_{t\to\infty} V = 0$. Finally, we have $\lim_{t\to\infty} S = \frac{\Lambda}{\mu}$ and thus $X_0$ is globally asymptotically stable.

□

**Proposition 6.2.3.** *The endemic equilibria of system* (22) *are:*

$$X_E = \Bigg(\frac{\Lambda(\mu+\gamma)}{\mu\beta}, \frac{\Lambda\theta^2\eta r_v}{\mu m r_i(\mu+\gamma)}, \frac{\Lambda\gamma\theta^2\eta r_v}{\mu m r_i(\mu+\gamma)(\mu+\psi)}, \frac{\Lambda m r_i(\beta-\mu-\gamma)(\mu+\gamma)(\mu+\psi) - \Lambda\beta\theta^2\eta r_v(\mu+\psi+\gamma)}{\mu\beta m r_i(\mu+\gamma)(\mu+\psi)}, \frac{\Lambda\theta r_v}{\mu r_i m}, \frac{\mu\beta(\mu+\phi)}{\Lambda\rho(\mu+\gamma)}V_E\Bigg)$$

$$X_E^* = \left(\frac{\Lambda(\mu+\gamma)}{\mu\beta}, \frac{\Lambda(\beta-\mu-\gamma)(\mu+\psi)}{\mu\beta(\mu+\psi+\gamma)}, \frac{\Lambda\gamma(\beta-\mu-\gamma)}{\mu\beta(\mu+\psi+\gamma)}, 0, \frac{\Lambda(\beta-\mu-\gamma)(\mu+\psi)(\mu+\gamma)}{\mu\beta\theta\eta(\mu+\psi+\gamma)}, 0\right)$$

$$\bar{X}_E = \left(\frac{\Lambda(\mu+\gamma)}{\mu\beta}, \frac{\Lambda(\mu+\psi)\big((\beta-\mu-\gamma)(\mu+\phi)-\rho(\mu+\gamma)\big)}{\mu\beta(\mu+\psi+\gamma)(\mu+\phi)}, \frac{\Lambda\gamma\big((\beta-\mu-\gamma)(\mu+\phi)-\rho(\mu+\gamma)\big)}{\mu\beta(\mu+\psi+\gamma)(\mu+\phi)}, \frac{\Lambda\rho(\mu+\gamma)}{\mu\beta(\mu+\phi)}, \frac{\mu\beta\bar{S}\bar{I}}{\Lambda\theta\eta}, 1\right).$$

*The endemic equilibria $X_E$ and $X_E^*$ exist if and only if $\mathcal{R}_0 = \frac{\beta}{\mu+\gamma} > 1$. The pure-vaccinator endemic equilibrium $\bar{X}_E$ exists if and only if $\mathcal{R}_0 > 1$ and $\rho < \frac{(\beta-\mu-\gamma)(\mu+\phi)}{\mu+\gamma}$. The pure non-vaccinator disease-free equilibrium $X_E^*$ is asymptotically stable for initial conditions $I_0 \neq 0$ if there exists a time $T$ such that*

$$r_v > \lim_{t\to\infty} \frac{\beta m r_i e^{-\eta t}}{N^2\theta^2} \int_T^t S(\tau)I(\tau)e^{\eta\tau}d\tau.$$

*Proof.* The existence of the endemic equilibria follows directly from the assumption that they must be non-negative. Next, we can ensure that if the risk of vaccination

is sufficiently high, individuals will cease vaccination behaviour. This requires that there exists some time $T$ for which $x'$ remains negative for all $t \geq T$. We are therefore looking for when

$$-r_v + \frac{mr_i M(t)}{N\theta} < 0.$$

We have that

$$\begin{aligned} M' &= \frac{1}{\theta}\left(\frac{\beta SI}{N} - \theta\eta M\right) \\ \eta M + M' &= \frac{\beta SI}{N\theta} \\ \eta M e^{\eta t} + M' e^{\eta t} &= \frac{\beta SI}{N\theta} e^{\eta t} \\ \frac{d}{dt}\left[M e^{\eta t}\right] &= \frac{\beta SI}{N\theta} e^{\eta t} \\ M &= \frac{\beta e^{-\eta t}}{N\theta} \int S(t) I(t) e^{\eta t} dt. \end{aligned} \tag{23}$$

Thus if there exists a time $T$ such that $r_v > \lim_{t\to\infty} \frac{\beta m r_i e^{-\eta t}}{N^2\theta^2} \int_T^t S(\tau) I(\tau) e^{\eta\tau} d\tau$, then we have $x' < 0$ on $[T, \infty)$. This ensures that $\lim_{t\to\infty} x = 0$, which removes imitation dynamics and memory from the model, reducing it to the $SIRS$ model from Chapter 2. Therefore under this condition the endemic equilibrium $X_E^*$ is globally asymptotically stable.

□

A similar condition cannot be derived in the same way for stability of the pure-vaccinator endemic equilibrium (with $r_v \neq 0$). This is due to the drop in disease prevalence in the memory of the population that occurs as solutions approach $\bar{X}_E$. This drop in disease prevalence reduces the risk of infection below the risk of vaccination, causing a decrease in vaccination coverage (similarly to the instability of the pure-vaccinator equilibrium of system (19)).

## 6.3 Numerical simulations and sensitivity analysis

### 6.3.1 Numerical simulations

Numerical simulations and graphs were created with Matlab using the Runge–Kutta (4,5) method with relative and absolute integration error tolerances set to $10^{-12}$ to ensure that solutions remain positive. The value of $x$ decreases to values close to zero, which causes the ODE solver to approximate the solution as being negative whenever disease prevalence is low for a significant portion of the memory span. Parameter values chosen for the simulations are provided in Table 7, unless otherwise specified, and were chosen from the values used in previous chapters. The results of these simulations are provided in Figures 20 and 21.

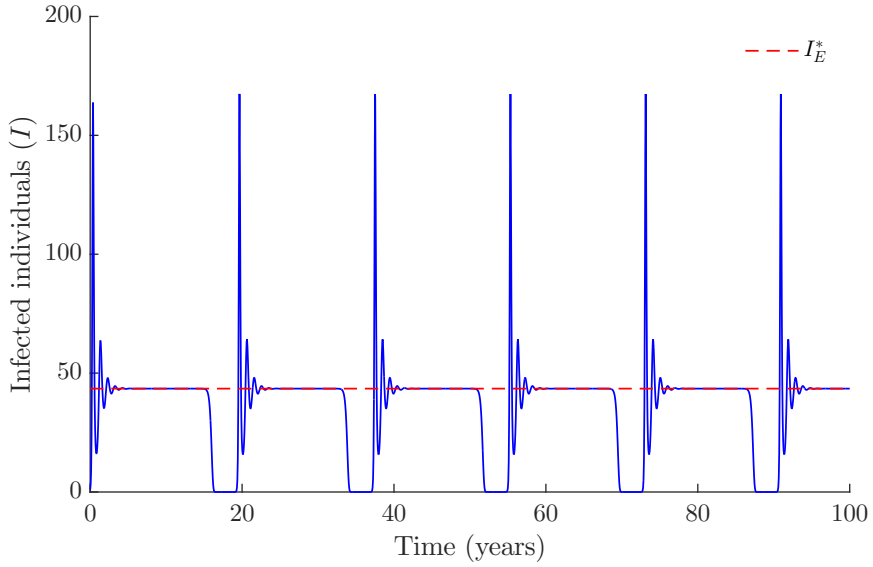


Figure 20: Time series of infected individuals ($I$) versus time with memory span $\theta = 3$ seasons. Solutions oscillate and remain positive for all time. Solutions approach the endemic equilibrium $X_E^*$ before losing stability through accumulation of infected individuals in the memory of the population.

In Figure 20, solutions act in a similar fashion to those of Chapter 3 until the

Table 7: Parameter values used for numerical simulations of system (8). Parameter values in this table are used for all simulations in this section unless otherwise stated.

| Parameter | Description | Simulation value | Ref. |
|---|---|---|---|
| $\mu$ | Human death rate | $\frac{1}{80 \cdot 365}$ | [46] |
| $\Lambda$ | Human birth rate | $10000\mu$ | Calculated |
| $\beta$ | Contact rate | 0.3 | [a] |
| $\gamma$ | Recovery rate | $\frac{1}{4}$ | Assumed[b] |
| $\psi$ | Rate of waning immunity (natural) | $\frac{1}{150}$ | [8][c] |
| $\phi$ | Rate of waning immunity (vaccine) | $\frac{1}{150}$ | [8][c] |
| $m$ | Sensitivity to prevalence | 0.8 | Assumed |
| $r_i$ | Risk of infection | 0.92 | Assumed[d] |
| $k$ | Mixed imitation rate | 1 | Assumed |
| $\rho$ | Vaccination rate | 0.05 | Assumed |
| $\theta$ | Length of memory span (seasons) | Varied | Assumed |

[a] Contact rate was chosen to give values of $\mathcal{R}_0 \in (1, 2)$.

[b] To be able to show periodic dynamics in a realistic time frame, the recovery time was decreased past the minimum five days of contagious infection [7].

[c] Rates of waning immunity (vaccine and naturally induced) were chosen to be equal and last for five months, corresponding to a month before and after peak activity.

[d]Risk of vaccination is excluded as $r_v = 1 - r_i$.

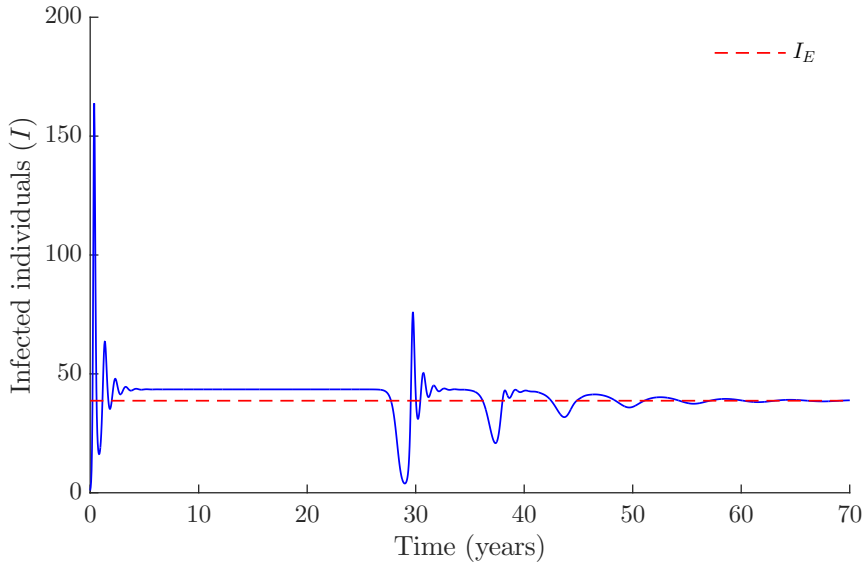


Figure 21: Time series of infected individuals ($I$) versus time with memory span $\theta = 3.25$ seasons. Solutions oscillate and approach the endemic equilibrium, denoted by the dashed red line.

memory of disease prevalence increases past the threshold value in the equation for $x'$, leading to a surge of vaccination. These figures correspond to a memory span of three years and risk of vaccination of $r_v = 0.08$ (higher than would be expected for seasonal influenza vaccination). Increasing the memory span stabilizes oscillations of solutions when all other parameters remain fixed; however, if the risk of vaccination is decreased sufficiently, periodic dynamics may be maintained. For example, when individuals had a memory span of ten years, a vaccination risk of $r_v = 0.02$ was sufficiently small to sustain recurrent epidemics (results omitted due to similarity with Figure 20). In Figure 21, we increased the length of memory to demonstrate the stabilizing effects of the memory mechanism. When the memory span was increased from three years to three and a quarter years, solutions stop oscillating and converge to the mixed-strategy endemic equilibrium $X_E$. In this case, the number of infections in the memory of the population is sufficient to ensure that the risk of vaccination is sufficiently high to maintain a demand for vaccinations.

Although we have chosen a lower risk of infection than would be expected for the general population, simulations with higher risk ($r_i = 0.999$) still exhibit periodic dynamics with a period length of over one hundred years (since solutions approach extremely close to $x = 1$ before coverage begins to fall). This result is similar for longer memory spans, which require higher infection risks. This shows that, as a disease nears eradication, voluntary vaccination campaigns are expected to fail. The free-rider dilemma thus poses a substantial issue for public health.

### 6.3.2 Sensitivity Analysis

We will again use Latin hypercube sampling and partial rank correlation coefficients to determine the sensitivity of the model to its parameters, with a sample size of $N = 1000$. As with the previous models, the expression for $\mathcal{R}_0$ for system (22) is too simple to provide a valuable output for a complete sensitivity analysis. We have thus chosen the output to be the number of infected individuals at the mixed-strategy endemic equilibrium ($I_E$) scaled by population size, similarly to Chapter 3. The results are shown in the Figures 22 and 23.

Parameter ranges were selected with the same method as in Chapters 3 and 5, with the exception of the vaccination rate. The vaccination rate spans the same ranges as Chapter 3 but is not scaled by the population size as was done in Chapter 3. The results of the sensitivity analyses were qualitatively similar to those of previous chapters with the contact rate ($\beta$) and the recovery rate ($\gamma$). The risk of infection as well as the length of memory span were just below a significant value to be considered sensitive parameters. The results are shown in Figure 23. The proportion of infected individuals at the mixed-strategy equilibrium is independent of the vaccination rate ($\rho$). To ensure that all parameters were studied, sensitivity analyses were also conducted on the value of $x_E$, which is dependent on the vaccination rate using the above method with minimum and maximum values of 0.005 and 0.6, respectively. It was found that $x_E$ was not sensitive to the vaccination rate. Results were omitted due to providing qualitatively similar results to Figures 22 and 23.

Table 8: Minimum and maximum values for PRCCs/LHS for Figures 22 and 23 using uniform distribution.

| Parameter | Minimum | Maximum | Parameter | Minimum | Maximum |
|---|---|---|---|---|---|
| $\mu$ | $\frac{1}{90\cdot365}$ | $\frac{1}{70\cdot365}$ | $r_i$ | 0.95 | 0.9999 |
| $\beta$ | 0.25 | 0.6 | $m$ | 0.5 | 1.5 |
| $\gamma$ | $\frac{1}{8}$ | $\frac{1}{4}$ | $\theta$ | 2 | 6 |
| $\psi$ | $\frac{1}{200}$ | $\frac{1}{100}$ | | | |

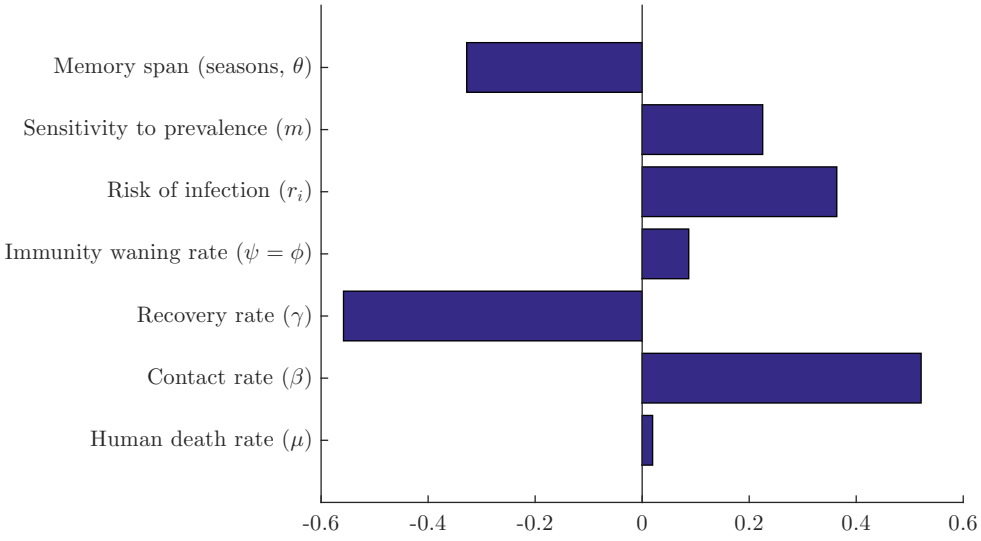


Figure 22: PRCC sensitivity analysis with $N = 1000$ simulations for listed parameters of system (22) using ranges from Table 8 and the number of infected individuals at the endemic equilibrium ($I_E$) as the output.

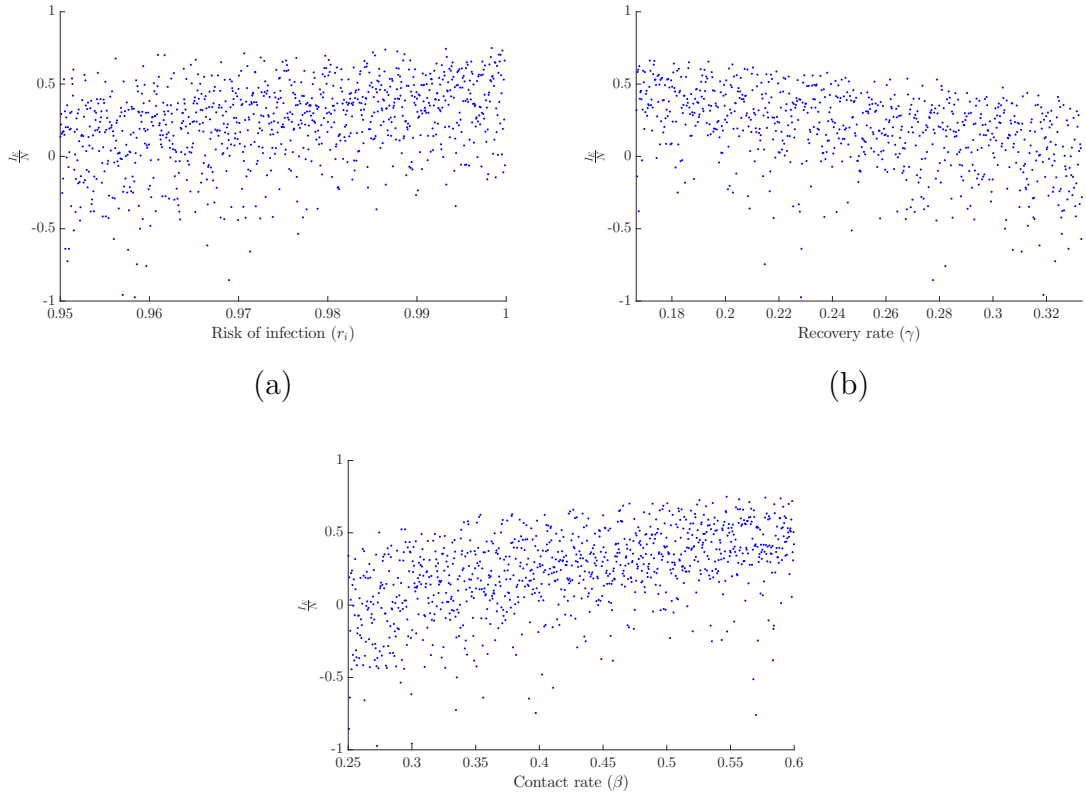


Figure 23: Dependence of $\frac{I_E}{N}$ on the three most sensitive parameters (determined from the PRCCs) of system (22): (a) risk of infection ($r_i$), (b) recovery rate ($\gamma$), (c) contact rate ($\beta$). Results were generated over $N = 1000$ simulations with parameter ranges shown in Table 8.

## 6.4 Discussion

Dynamics of particular interest are the periodic dynamics shown in Figure 16. The time-series approaches the endemic equilibrium through oscillations similar to a standard SIRS model with vaccination. However, if at the endemic equilibrium the number of new infectious cases per day accumulates over some threshold level, the perceived risk of infection will provide a higher payoff, causing a switch in behaviours. Through vaccination, disease prevalence drops towards zero, which in turn decreases

the number of cases in the memory mechanism, causing a second switch in behaviour and triggering another epidemic. In comparison to the model in Chapter 3, the model with both imitation dynamics and memory allows for periodic dynamics for larger memory spans as long as the risk of vaccination was perceived as being sufficiently low. Where this model lacks realism is that individuals do not seek vaccination unless there has been a high number of infections in their memory. This leads to scenarios in which strong vaccination coverage is only obtained for a period of one to two years before returning towards zero. Although this may not be realistic for the current status of influenza immunization and infection, it shows that, as prevalence of disease decreases near an eradication threshold, individuals may stop protecting themselves through vaccination (or other protection methods such as social distancing), as it would come at a higher individual cost. These results suggest that diseases controlled by voluntary vaccination campaigns cannot be eradicated without other preventative measures. This idea has been corroborated by several studies [3, 30, 44, 48]. Influenza is a particularly difficult disease to eradicate, as the vaccine is limited to a single season of use. Introduction of a universal flu vaccine has also been suggested to not be capable of eradicating influenza, and our results corroborate these claims. Since the risk of vaccination relative to the risk of infection increases as prevalence decreases, individuals receive a higher payoff by free-riding on herd immunity. Once a sufficiently large pool of susceptible individuals is present, the disease will re-emerge. Re-emergence of currently controlled vaccine-preventable diseases such as measles (which has already caused new outbreaks) and polio could be possible as prevalence decreases; control methods must be maintained. We would like to note that these results do not suggest that mandatory vaccinations should be put in place to combat vaccine-preventable diseases, as they impede on human rights and would be expected to come with stern societal opposition. Instead, efforts in reducing new strains of influenza by decreasing human contact with infected animal reservoirs such as concentrated animal feeding operations (CAFO) or vaccination of CAFO workers should be considered. Public education must also be used to ensure that individuals understand the importance of hygienic practices that reduce transmission of influenza, such as washing hands and covering the mouth and nose when coughing or sneezing.

Epidemiological models have provided a vast wealth of knowledge on the spread of disease in our population. However, the very nature of these models assumes that individuals act the same at any given time; human behaviour is far from uniform. It is important that future studies into disease models include a discussion regarding human behaviour whenever a control parameter is introduced that is enacted at the individual level. For example, a study that shows that disease prevalence decreases through social distancing should also evaluate the willingness of individuals to adopt an altered behaviour (such a model has already been studied and provides similar results to the models in this paper [31]). The difficulty in implementing this is estimating the perceived costs of the control measures at the individual level.

In conclusion, when individuals act to reduce disease prevalence with self-interest, diseases may resurface following successful vaccination campaigns. For diseases that rely on voluntary vaccination campaigns, a second phase of action must be planned to ensure eradication of a disease through measures such as the role that ring vaccination played in the eradication of smallpox. Although influenza would not be able to be eradicated through the current seasonal vaccination campaigns (with new variants arising each season), if and when a universal vaccine is developed, public-health officials will need to create a detailed plan on ways to limit transmission of influenza to complement current voluntary vaccination policies.

# Chapter 7

# Results, conclusions and future work

Integrating evolutionary game theory into disease models with individual-based decisions allows us to study the free-rider dilemma. Classic mass-vaccination does not accurately model voluntary vaccination and lacks the ability to describe the limitations of voluntary vaccination programs caused by individuals free-riding on herd immunity.

The results of Chapter 4 suggest that the free-riding dilemma leads to sub-optimal vaccination coverage in regards to the group optimum when individuals act with self-interest, corroborating the findings of previous research [3, 4, 12, 13, 24]. Although the model relies on a fixed equilibrium point to determine the Nash equilibrium, it shows that the increases in payoff and the probability of vaccination are marginal for diseases with low reproductive ratios, such as influenza. The goal set by the Government of Canada for seasonal influenza vaccination by 2010 was a coverage level of 80%, although only an estimated 37.2% of the population received influenza vaccination in the 2012 [33]. Future research should determine whether these coverage goals are attainable and if education campaigns aimed at attaining these goals are cost-effective. Our results suggest that these coverage goals may be unrealistic due to individual-based vaccination decisions and the marginal increases in vaccination coverage following education campaigns.

The static nature of the game-theoretic model of Chapter 4 motivated the need to study a dynamic game in which individuals respond to the prevalence of infection and the vaccination behaviour of the population. Utilizing evolutionary game theory through imitation dynamics in Chapter 5 allowed for periodic oscillations for high infection risk (and hence low vaccination risk) consistent with the risk of influenza vaccines relative to influenza infection. The definition of an evolutionary stable strategy would need to be extended to be consistent with periodic dynamics, due to the natural oscillations of influenza from seasonal forcing and changes in vaccination behaviour. Although we cannot determine the evolutionary stable strategy with the current definition, imitation dynamics provide a basic mechanism to study the effects of human behaviour on disease intervention efforts. The observed oscillations were also found in Chapter 6, with the inclusion of the exponentially fading memory mechanism used in Chapter 3. This model allowed for longer memory spans while maintaining periodic dynamics. This suggests that populations become susceptible to subsequent epidemics as the prevalence of disease decreases through successful vaccination campaigns. This feedback mechanism could partially explain the resurgence of measles in developed countries such as the UK and the United States. Furthermore, it reinforces the need for maintaining control efforts as a disease approaches eradication. Our results suggest voluntary vaccination campaigns would not be successful at maintaining low prevalence indefinitely and that models of control mechanisms that do not consider individual-based decisions could lead to an overestimation in the efficacy of disease-control programs.

The results of the previous chapters suggest that it may be impossible to eradicate diseases with a low reproductive ratio such as influenza through voluntary vaccination campaigns. Our models provide limited results, since the populations considered were homogeneous, while it is well known that influenza infection risk is increased for seniors, infants and immunocompromised individuals [7]. It is also expected that individuals imitate individuals more often from their own age group, consistent with regular contact patterns of a population. This would require further study.

Future work will include the elaboration of the notion of an evolutionary stable strategy for periodic dynamics and extending imitation dynamics to a heterogeneous

population. Determining factors that can control the spread of influenza A without the need for individual-based decisions such as vaccination, social-distancing or hygienic practices should be analyzed in detail. The difficulty posed by controlling influenza A is the large animal reservoir that allows it to undergo antigenic shift and successfully evade our immune system. Concentrated animal-feeding operations (CAFO) allow for the virus to spread easily between livestock and CAFO workers. We may be able to limit the spread of influenza within our livestock by reducing their density on CAFO farms, effectively reducing their contact rate. In this way, we limit the reproduction rate of the influenza virus within livestock and consequently decrease the rate of establishment of new genetic variants of influenza through antigenic shift. Elaborate in-host models will need to be constructed in order to test these hypotheses and determine whether or not changing international policy for concentrated animal-feeding operations to limit the density of livestock would reduce the transmission of lethal genetic variants influenza A (such as avian influenza). Proactive methods capable of reducing influenza transmission that are not sensitive to human behaviour should be considered. Integrating such methods with current voluntary influenza vaccination policies could prove beneficial in reducing the risk of global influenza related morbidity and mortality.

# Bibliography


[1] C.T. Bauch, *Imitation dynamics predict vaccination behaviour*, Proceedings of the Royal Society, Vol. 272, 1669-75 [2005].

[2] C.T. Bauch and S. Battacharyya, *Evolutionary game theory and social learning can determine how vaccine scares unfold*, PLOS Computational Biology, Vol 8:4 [2012].

[3] C.T. Bauch, D.J.D Earn, *Vaccination and the theory of games*, Proceedings of the National Academy of Sciences of the United States of America, Vol. 101:13, 13391-94 [2004].

[4] C.T. Bauch, A.P. Galvani, D.J.D Earn, *Group interest versus self-interest in smallpox vaccination policy*, Proceedings of the National Academy of Sciences of the United States of America, Vol. 100:18, 10564-67 [2003].

[5] M. Biggerstaff, S. Cauchemez, C. Reed, M. Gambhir, L. Finelli, *Estimates of the reproduction number for seasonal, pandemic, and zoonotic influenza: a systematic review of the literature*, BMC Infectious diseases, Vol. 14:1, 480 [2014].

[6] S.M. Blower, H. Dowlatabadi, *Sensitivity and uncertainty analysis of complex models of disease transmission: and HIV model, as an example*, International statistical Review, Vol. 62:2, 229–43, [1994].

[7] CDC, NCIRD, *Key Facts about Influenza (Flu)*, Centers for Disease Control and Prevention, [http://www.cdc.gov/flu/keyfacts.htm].

[8] CDC, NCIRD, *The Flu Season*, Centers for Disease Control and Prevention,[http://www.cdc.gov/flu/about/season/flu-season.htm].

[9] D.M. Cornforth, T.C. Reluga, E. Shim, C.T. Bauch, A.P. Galvani, L.A. Meyers, *Erratic Flu Vaccination Emerges from Short-Sighted Behavior in Contact Networks*, PLoS Computational Biology, Vol. 7:1, [2011].

[10] F.S. Dawood, A.D. Iuliano, C. Reed, M.I. Meltzer, D.K. Shay et al., *Estimated Global Mortality Associated with the First 12 Months of 2009 Pandemic Influenza A H1N1 Virus Circulation: A Modelling Study*, The Lancet Infectious Diseases, Vol.12:9, 687-95, [2012].

[11] J.C. Eckalbar, W.L. Eckalbar, *Dynamics of an SIR model with vaccination dependent on past prevalence with high-order distributed delay*, BioSystems, Vol. 129, 50–65, [2015].

[12] P.E.M. Fine and J.A. Clarkson, *Individual versus public priorities in the determination of optimal vaccination policies*, American Journal of Epidemiology Vol. 126:6, 1012-20 [1986].

[13] A.P. Galvani, T.C. Reluga, G.B. Chapman, *Long-standing influenza vaccination policy is in accord with individual self-interest but not with the utilitarian optimum*, Proceedings of the National Academy of Sciences of the United States of America, Vol. 104:13, 5692-97 [2007].

[14] N.C Grassly, C. Fraser, *Seasonal infectious disease epidemiology*, Proceedings of the Royal Society, Vol. 273, 2541–50, [2006].

[15] N.A. Halsey, D.A. Salmon, *Measles at Disneyland, a Problem for All Ages*, Annals of Internal Medicine, Vol. 162:9, 655–56, [2015].

[16] A.A. Jansen, N. Stollenwerk, H.J. Jensen, M.E Ramsay, W.J. Edmunds, C.J. Rhodes, *Measles outbreaks in a population with declining vaccine uptake*, Science, 804, [2003].

[17] A. Kata, *A postmodern Pandora's box: Anti-vaccination misinformation on the Internet*, Vaccine, Vol. 28, 1709-16 [2010].

[18] W. Kermack, A. McKendrick, *Contributions to the mathematical theory of epidemics*, Bulletin of Mathematical Biology, Vol. 53, 33–55, [1991].

[19] A.M. Lyapunov, *General problem of the stability of motion*, Tayor & Francis, [1992].

[20] M.D. Mckay, R.J Beckman, W.J. Conover, *A Comparison of Three Methods for Selecting Values of Input Variables in the Analysis of Output from a Computer Code*, Technometrics, Vol. 42:1,55, [2000].

[21] S. Merler, M. Ajelli, *The role of population heterogeneity and human mobility in the spread of pandemic influenza*, Proceedings of the Royal Society, Vol. 277, 557–65, [2009].

[22] J.M. Nagata, I. Hernndez-Ramos, A. Sivasankara Kurup, D. Albrecht, C. Vivas-Torrealba, C. Franco-Paredes, *Social determinants of health and seasonal influenza vaccination in adults65 years: a systematic review of qualitative and quantitative data*, BMC Public Health, Vol. 13:388, [2013].

[23] J.F. Nash, *Equilibrium points in n-Person games*, Proceedings of the National Academy of Sciences of the United States of America, Vol. 36, 48–49, [1950].

[24] M.L. Ndeffo Mbah, J. Liu, C.T. Bauch, Y.I. Tekel, J. Medlock, L.A. Meyers, A.P. Galvani, *The Impact of Imitation on Vaccination Behavior in Social Contact Networks*, PLoS Computational Biology, Vol. 8:4, [2012].

[25] S.M. O'Regan, T.C. Kelly, A. Korobeinikov, M.J.A. OCallaghan, A.V. Pokrovskii, *Lyapunov functions for SIR and SIRS epidemic models*, Applied Mathematics Letters, Vol. 23:4, 446-48 [2010].

[26] C.W. Olsen, L. Brammer, B.C. Easterday, N. Arden, E. Belay, I. Baker, N.J. Cox, *Serologic Evidence of H1 Swine Influenza Virus Infection in Swine Farm*

*Residents and Employees*, Emerging Infectious Diseases, Vol. 8:8, 814–819, [2002].

[27] A. d'Onofrio, P. Manfredi, P. Poletti, *The impact of vaccine side effects on the natural history of immunization programmes: an imitation-game approach*, Journal of Theoretical Biology, Vol. 273:1, 63, [2011].

[28] A. d'Onofrio, P. Manfredi, E. Salinelli, *Vaccinating behaviour, information, and the dynamics of SIR vaccine preventable diseases*, Theoretical Population Biology, Vol. 71, 301–317, [2007].

[29] S.B. Omer, D.A. Salmon, W.A. Orenstein, M.P. deHart, N. Halsey, *Vaccine Refusal, Mandatory Immunization, and the Risks of Vaccine-Preventable Diseases*, The New England Journal of Medicine, Vol. 360, 1981–88, [2009].

[30] A. Perisic, C.T. Bauch, *Social Contact Networks and Disease Eradicability under Voluntary Vaccination*, PLoS Computational Biology, Vol. 5:2, [2009].

[31] P.Poletti, M. Ajelli, S. Mercier, *The Effect of Risk Perception on the 2009 H1N1 Pandemic Influenza Dynamics*, PLoS ONE, Vol. 6:2 [2011].

[32] Public Health Agency of Canada, *Influenza Virus Type A: Pathogen Safety Data Sheet - Infectious Substances*, [http://www.phac-aspc.gc.ca/lab-bio/res/psds-ftss/influenza-a-eng.php].

[33] Public Health Agency of Canada, *Vaccine coverage amongst adult Canadians: Results from the 2012 adult National Immunization Coverage (aNIC) survey*, [http://www.phac-aspc.gc.ca/im/nics-enva/vcac-cvac-eng.php].

[34] F. Ramponi, *Notes On Lyapunov's Theorem*, [http://control.ee.ethz.ch/ifalst/docs/lyapunov.pdf].

[35] T.A. Reichert, N. Sugaya, D.S. Fedson, W.P. Glezen, L. Simonsen, M. Tashiro, *The Japanese Experience with Vaccinating Schoolchildren against Influenza*, New England Journal of Medicine, Vol. 344:12, 889-96 [2001].

[36] J. Renze, E.W. Weisstein, *Extreme Value Theorem*, MathWorld, [http://mathworld.wolfram.com/ExtremeValueTheorem.html].

[37] R.A. Saenz, H.W. Hethcote, G.C. Gray, *Confined Animal Feeding Operations as Amplifiers of Influenza*, Vector Borne Zoonotic Diseases, Vol. 6:4, 338-346, [2006].

[38] E. Shim, G.B. Chapman, J.P. Townsend, A.P. Galvani, *The influenza of altruism on influenza vaccination decisions*, Journal of the Royal Society Interface, Vol. 9, 2234–2243, [2012].

[39] J.M Smith and G.R Price, *The logic of animal conflict*, Nature Vol. 246, 15-18 [1973].

[40] C. Taylor, D. Fudenberg, A. Sasaki, M.A. Nowak, *Evolutionary game dynamics in finite populations*, Bulletin of Mathematical Biology, Vol. 66:6, 1621–1644, [2004].

[41] J. Treanor, *Influenza vaccine–outmaneuvering antigenic shift and drift*, New England Journal of Medicine, Vol. 350:3, 218-20 [2004].

[42] A. Trilla, G. Trilla, C. Daer, *The 1918 "Spanish Flu" in Spain*, Clinical Infectious Diseases Vol. 47:5, 668–673, [2008].

[43] R. Vardavas, R. Breban, S. Blower, *A universal long-term flu vaccine may not prevent severe epidemics*, BMC Research Notes, Vol. 3:92, [2010].

[44] R. Vardavas, R. Breban, S. Blower, *Can Influenza Epidemics Be Prevented by Voluntary Vaccination?*, PLoS Computational Biology, Vol. 3:5, [2007].

[45] C.R. Wells, C.T. Bauch, *The impact of personal experience with infection and vaccination on behaviour-incidence dynamics of seasonal influenza*, Epidemics, Vol. 4, 139–151, [2012].

[46] World Health Organization, *World Health Statistics 2016: Monitoring health for the SDGs Annex B: tables of health statistics by country, WHO region and globally*, WHO, [2016].

[47] A. Wolf, J.B. Swift, H.L. Swinney, J.A. Vastano, *Determining Lyapunov Exponents from a Time Series*, Physica, Vol. 16, 285–317, [1985].

[48] B. Wu, F. Fu, L. Wang, *Imperfect Vaccine Aggravates the Long-Standing Dilemma of Voluntary Vaccination*, PLoS ONE, Vol. 6:6, [2011].

[49] Y. Xie, J. Gong, M. Li, H. Fang, W. Xu, *The medicinal potential of influenza virus surface proteins: hemagglutinin and neuraminidase*, Current Medicinal Chemistry, Vol. 18:7, 1050-66, [2011].

[50] M.C. Zambon, *Epidemiology and pathogenesis of influenza*, Journal of Antimicrobial Chemotherapy, Vol. 44:90002, 3-9 [1999].